

IMPROVING QUALITY OF CVD GRAPHENE GROWN ON  
THE COPPER FOIL BY PHYSICAL  
POLISHING ELECTROPOLISHING AND THERMAL  
ANNEALING PRETREATMENT PROCESSES



A Thesis Submitted in Partial Fulfillment of the Requirements  
for the Degree of Master of Science in Nanoscience and Technology  
(Interdisciplinary Program)  
Inter-Department of Nanoscience and Technology  
GRADUATE SCHOOL  
Chulalongkorn University  
Academic Year 2022  
Copyright of Chulalongkorn University

การปรับปรุงคุณภาพของซีวีดีกราฟิฟที่ปลุกบนฟอยล์ทองแดงโดยกระบวนการเตรียมก่อนปลุกด้วย  
การขัดเชิงกายภาพ การขัดด้วยเคมีไฟฟ้าและการอบด้วยความร้อน



วิทยานิพนธ์นี้เป็นส่วนหนึ่งของการศึกษาตามหลักสูตรปริญญาวิทยาศาสตรมหาบัณฑิต  
สาขาวิชาวิทยาศาสตร์นาโนและเทคโนโลยี (สหสาขาวิชา) สหสาขาวิชาวิทยาศาสตร์นาโนและ  
เทคโนโลยี

บัณฑิตวิทยาลัย จุฬาลงกรณ์มหาวิทยาลัย

ปีการศึกษา 2565

ลิขสิทธิ์ของจุฬาลงกรณ์มหาวิทยาลัย

Thesis Title	IMPROVING QUALITY OF CVD GRAPHENE GROWN ON THE COPPER FOIL BY PHYSICAL POLISHING ELECTROPOLISHING AND THERMAL ANNEALING PRETREATMENT PROCESSES
By	Mr. Methawut Sirisom
Field of Study	Nanoscience and Technology (Interdisciplinary Program)
Thesis Advisor	Associate Professor SAKUNTAM SANORPIM, Ph.D.
Thesis Co Advisor	WARAKORN YANWACHIRAKUL, Ph.D.

---

Accepted by the GRADUATE SCHOOL, Chulalongkorn University in Partial Fulfillment of the Requirement for the Master of Science

.....  
Dean of the GRADUATE SCHOOL  
(Associate Professor YOOTTHANA CHUPPUNNARAT, Ph.D.)

THESIS COMMITTEE

..... Chairman  
(Assistant Professor RATTHAPOL RANGKUPAN, Ph.D.)  
..... Thesis Advisor  
(Associate Professor SAKUNTAM SANORPIM, Ph.D.)  
..... Thesis Co-Advisor  
(WARAKORN YANWACHIRAKUL, Ph.D.)  
..... Examiner  
(Rongrong Cheacharoen, Ph.D.)  
..... External Examiner  
(Assistant Professor PAWINEE KLANGTAKAI, Ph.D.)



จุฬาลงกรณ์มหาวิทยาลัย  
CHULALONGKORN UNIVERSITY

เมธาวุฒิ ศิริโสม : การปรับปรุงคุณภาพของชีวิติกราฟีนที่ปลูกบนฟอยล์ทองแดงโดยกระบวนการเตรียมก่อนปลูกด้วยการขัดเชิงกายภาพ การขัดด้วยเคมีไฟฟ้าและการอบด้วยความร้อน. ( IMPROVING QUALITY OF CVD GRAPHENE GROWN ON THE COPPER FOIL BY PHYSICAL POLISHING ELECTROPOLISHING AND THERMAL ANNEALING PRETREATMENT PROCESSES) อ.ที่ปรึกษาหลัก : รศ. ดร.ศกฤชธรรม เสนาะพิมพ์, อ.ที่ปรึกษาร่วม : ดร.วรากร ญาณวชิรากุล

การศึกษานี้ได้ทำการปรับปรุงกระบวนการเตรียมพื้นผิวก่อน (การขัดผิวเชิงกายภาพ, การขัดผิวด้วยเคมีไฟฟ้า, และการอบด้วยความร้อน) เพื่อเพิ่มคุณภาพของกราฟีนที่เติบโตบนฟอยล์ทองแดง (Cu) ที่มีความบาง โดยใช้สาร Brasso เพื่อปรับผิวให้เรียบ จากนั้นขัดผิวด้วยเคมีไฟฟ้า ใช้  $H_3PO_4$  เพื่อลดรีวรอยบนพื้นผิวฟอยล์ทองแดง กระบวนการขัดผิวเคมีไฟฟ้า ใช้  $H_3PO_4$  ที่มีความเข้มข้นที่แตกต่างกันในช่วง 30-60% และเวลาในช่วง 60-120 วินาที หลังจากนั้น ฟอยล์ทองแดงถูกอบด้วยความร้อน ที่อุณหภูมิ 860-940 °C กราฟีนถูกปลูกผลึกด้วยวิธี CVD โดยใช้  $C_6H_{12}$  เป็นสารตั้งต้นของคาร์บอน และ  $N_2$  เป็นก๊าซนำพา ผิวฟอยล์ทองแดงที่ได้ปรับให้เหมาะสมด้วยการบวมการขัดเชิงกายภาพและการขัดด้วยเคมีไฟฟ้าด้วย ที่ใช้ความเข้มข้นของ  $H_3PO_4$  ที่ 45% และเวลา 90 วินาที และการอบด้วยความร้อนที่อุณหภูมิ 900 °C ฟอยล์ทองแดงที่ผ่านกระบวนการข้างต้นทำให้ได้กราฟีนชั้นเดียวเติบโตสำเร็จ แต่ต้องใช้ปริมาตร  $C_6H_{12}$  น้อยลง มีอัตราส่วน  $I_{2D}/I_G$  สูงที่สุดเป็น 2.76 ผลการวิจัยนี้เน้นความสำคัญของอุณหภูมิที่ใช้ในกระบวนการอบด้วยความร้อน และปริมาตรสารตั้งต้นของคาร์บอน  $C_6H_{12}$  ในการควบคุมคุณภาพฟิล์มกราฟีนบนฟอยล์ทองแดง

จุฬาลงกรณ์มหาวิทยาลัย  
CHULALONGKORN UNIVERSITY

สาขาวิชา	วิทยาศาสตร์นาโนและเทคโนโลยี (สหสาขาวิชา)	ลายมือชื่อนิสิต .....
ปีการศึกษา	2565	ลายมือชื่อ อ.ที่ปรึกษาหลัก .....
		ลายมือชื่อ อ.ที่ปรึกษาร่วม .....

# # 6388028420 : MAJOR NANOSCIENCE AND TECHNOLOGY  
(INTERDISCIPLINARY PROGRAM)

KEYWORD Graphene; electro-polishing; Thermal annealing; Cyclohexane;  
D: Direct-Liquid-Injection Chemical vapor deposition; Raman  
scattering

Methawut Sirisom : IMPROVING QUALITY OF CVD GRAPHENE  
GROWN ON THE COPPER FOIL BY PHYSICAL  
POLISHING ELECTROPOLISHING AND THERMAL ANNEALING  
PRETREATMENT PROCESSES. Advisor: Assoc. Prof. SAKUNTAM  
SANORPIM, Ph.D. Co-advisor: WARAKORN YANWACHIRAKUL,  
Ph.D.

This study optimized the pretreatment processes (physical polishing (PP), electropolishing (EP), and thermal annealing) for high-quality graphene growth on thin copper (Cu) foils. PP using Brasso solvent was applied to smoothen the substrate surface, followed by EP with  $H_3PO_4$  to reduce rolling lines and surface contamination. The EP process involved different  $H_3PO_4$  concentrations (30-60%) and etching times (60-120 seconds). After thermal annealing at 860-940 °C, graphene growth was performed using direct-liquid-injection chemical-vapor deposition with cyclohexane ( $C_6H_{12}$ ) as the carbon precursor and nitrogen as the carrier gas. The optimized conditions involved PP and EP with 45%  $H_3PO_4$  concentration and 90 seconds etching. At an annealing temperature of 900 °C, monolayer graphene was successfully formed. Lower cyclohexane flow rates enhanced graphene quality, achieving monolayer films with an  $I_{2D}/I_G$  ratio of 2.76 for a 10-minute growth. By optimizing growth conditions, the graphene film properties were improved. These findings highlight the importance of annealing temperature and cyclohexane flow rates in controlling graphene film quality on Cu foils, providing valuable insights for graphene synthesis in various applications.

จุฬาลงกรณ์มหาวิทยาลัย  
CHULALONGKORN UNIVERSITY

Field of Study: Nanoscience and  
Technology  
(Interdisciplinary  
Program)

Academic  
Year:

2022

Student's Signature

.....

Advisor's Signature

.....

Co-advisor's Signature

## ACKNOWLEDGEMENTS

I wish to express my sincere gratitude to my advisor, Associate Professor Dr. Sakuntam Sanorpim, and my co-advisor, Dr. Warakorn Yanwachirakun, for their invaluable guidance and unwavering support throughout this thesis. Their insightful suggestions and dedication have been instrumental in shaping my work during my Master's study.

I am deeply appreciative of the attention and enriching experiences they have provided me, which have been fundamental to my academic growth.

I extend my heartfelt thanks to my thesis committee, Assistant Professor Dr. Rattapol Rangkupan, Dr. Rongrong Cheacharoen, and Assistant Professor Dr. Pawinee Klangtakai, for their valuable comments on my thesis, which have contributed to its refinement.

A special acknowledgment goes to Miss Charin Seesomdee, the Program Coordinator in Nanoscience and Technology, for her assistance with academic documents during my time in the program.

I am also grateful to my colleagues from AMPRG, with particular thanks to Assistant Professor Dr. Sukkaneste Tungasmita for engaging discussions and enjoyable moments shared.

I would like to acknowledge the support of the Graduate School and Department of Physics, Faculty of Science, Chulalongkorn University, and the Thailand Research Fund (Grant no. RSA5480025) for making this research possible.

Finally, I want to express deep and heartfelt appreciation to my father, mother, and kind uncle for their unwavering love, understanding, and encouragement throughout this long journey. Their support has been the pillar that kept me going.

Methawut Sirisom

# TABLE OF CONTENTS

	<b>Page</b>
.....	iii
ABSTRACT (THAI) .....	iii
.....	iv
ABSTRACT (ENGLISH).....	iv
ACKNOWLEDGEMENTS.....	v
TABLE OF CONTENTS.....	vi
LIST OF TABLES.....	1
LIST OF FIGURES .....	1
CHAPTER I.....	1
INTRODUCTION .....	1
1.1 Overview.....	1
1.2 Overview.....	4
1.3 Expectation .....	4
1.4 Organization of the thesis .....	4
CHAPTER II.....	6
BACKGROUND AND TREORY.....	6
2.1 Structural and property of graphene .....	6
2.1.1 Structural property.....	6
2.1.2 Crystal structure .....	6
2.1.2 Electrical property .....	9
2.2 Substate preparation and graphene growth process.....	10
2.2.1 Substate preparation .....	10
2.2.1.1 Electro-chemical polishing.....	10
2.2.1.2 Annealing process.....	13
2.2.3 Graphene growth process .....	13

2.2.3.1 Chemical Vapor Deposition.....	13
2.2.3.2 Direct Liquid Injection Chemical Vapor Deposition.....	14
2.3 Characterization of graphene .....	15
2.3.1 Optical microscope.....	15
2.3.1 X-ray diffraction.....	16
2.3.2 Raman spectroscopy.....	16
2.3.3 Raman band of graphene.....	18
G band	20
D band	20
2D band .....	20
D' and 2D' band.....	21
CHAPTER III .....	23
EXPERIMENTAL DETIALS.....	23
3.1 Optimization the copper foil surface for graphene growth.....	23
3.1.1 Electro-polishing process .....	23
3.1.2 Annealing process.....	25
3.1.3 Graphene growth process .....	26
3.2 Growth of graphene by DLI-CVD method by cyclohexane precursor in N <sub>2</sub> gas carrier.....	28
3.2.1 DLI-CVD growth process .....	28
3.2.2 Characterization Methods.....	29
CHAPTER IV .....	30
RESULTS AND DICUSSIONS.....	30
4.1 Optimization of pretreatment processes for graphene synthesis .....	30
4.1.1 The effects of treatment process to Cu foil surface .....	31
4.1.2 The thermal annealing process effects. ....	35
4.1.2.1 Structural properties of Cu foil surface by heat treatment. ....	35
4.1.2.1 The effect of annealing process on graphene growth process. ....	36
CHAPTER V .....	46



CONCLUSION.....	46
5.1 Conclusion.....	46
REFERENCES .....	2
VITA .....	6



## LISH OF TABLES

Page

Table 1 Parameters of graphene growth by DLI-CVD .....	28
--	----



## LIST OF FIGURES

	Page
Figure 1 Surface height of Cu foil after 120 s of electropolishing in a 50% H <sub>3</sub> PO <sub>4</sub> solution, with an RMS roughness of 0.9 nm. [26].....	4
Figure 2 Structural differences between graphite and graphene.....	8
Figure 3 Carbon diagram depicting sp <sup>2</sup> hybridization, adapted from. [29] .....	8
Figure 4 Schematic representation of the graphene lattice, and b) reciprocal lattice of the graphene lattice. ....	9
Figure 5 Band structure of graphene's $\pi$ -Bond (Conduction and Valence bands). [40] .....	10
Figure 6 Schematic representation of the electropolishing process of Cu foil substrate. ....	12
Figure 7 J-V characteristic of the electropolishing process. ....	12
Figure 8 Growth mechanism of graphene by CVD on metal substrates: Elementary steps for graphene growth on a catalytic substrate. ....	14
Figure 9 Schematic illustration of the X-ray diffraction process.....	17
Figure 10 Schematic of Raman scattering process. ....	18
Figure 11 Positions of D, G, and 2D bands in the Raman shift of graphene structure .....	19
Figure 12 Schematic illustration of the translational process of D, G, and 2D bands, adapted from [34].....	22
Figure 13 I-V performance for the electropolishing process at different concentrations of H <sub>3</sub> PO <sub>4</sub> . [26].....	24
Figure 14 Optimization of RMS surface roughness of Cu foil at 40%, 50%, and 60% H <sub>3</sub> PO <sub>4</sub> concentrations. [26].....	25
Figure 15 Flowchart of the experiment illustrating pretreatment and growth process. ....	27
Figure 16 Profile of the growth process.....	29
Figure 17 Optical image of the untreated Cu foil surface.....	31

Figure 18 Optical images of Cu foils after electropolishing with varying concentrations of phosphoric acid ( $H_3PO_4$ ) (30%, 40%, 50%, and 60%) for 90 seconds.....	33
Figure 19 Optical images of Cu foils obtained from the electropolishing (EP) process with 45% $H_3PO_4$ concentration, comparing the results with and without Brasso polishing after EP, depicting different dipping times of 60, 90, and 120 seconds. ....	35
Figure 20 Crystal orientation of Cu foil substrate: a) XRD intensity of Cu foil at different annealing temperatures, b) XRD intensity of Cu foil after the growth process with the same annealing temperature.....	38
Figure 21 Raman results of graphene on treated Cu foil: a) Graphene peaks at different annealing temperatures, b) $I_{2D}/I_G$ and $I_D/I_G$ ratio at different annealing temperatures.....	39
Figure 22 Raman spectra of graphene annealed at various temperatures: a) Zoomed-in 2D peaks with single Lorentzian fit (solid black line) at different annealing temperatures, b) Full Width at Half Maximum (FWHM) of D and 2D peaks at different annealing temperatures.....	41
Figure 23 Optical image of graphene film on Cu foil, showing Raman spot measurement positions (1-red solid lines and 2-blue dotted lines), along with a table displaying the temperature and time duration of annealing and graphene growth. b) Normalized Raman spectra of graphene obtained at positions 1 and 2. ....	43
Figure 24 Intensity ratio of 2D to G peak in graphene films on Cu foils as a function of growth time (1 to 6 minutes) at different annealing temperatures.....	43
Figure 25 Raman spectra of graphene films on Cu foils at various flow rates (0.1, 0.3, and 0.5 g/min) of cyclohexane. b) Optical images of graphene films on Cu foils corresponding to different flow rates (0.1, 0.3, and 0.5 g/min) of cyclohexane.....	45

# CHAPTER I

## INTRODUCTION

### 1.1 Overview

Graphene has attracted by researchers due to the two-dimensional monolayer material includes carbon atoms on hexagonal crystal structure that is unique physical properties, such as high thermal and electrical conductivity, high modulus of elasticity [1, 2] and high transparency [3]. To the unique properties used to various application for example optoelectronics [4, 5], sensor [6], super-capacitor [7] and solar cells [8]. Therefore, some devices required a high quality and large area of graphene materials for support their high potential in applications.

Chemical vapor deposition (CVD) is an efficient method for the preparation of large area and high-quality of graphene materials that includes several factors to consider in the monolayer graphene growth, along with thermodynamic and kinetic parameters, as well as type of precursor material and substrate. Firstly, the precursors for graphene synthesis, traditional CVD technique is usually grown graphene film using methane gas ( $\text{CH}_4$ ) as a carbon precursor which is high-quality large area graphene as well as acetylene ( $\text{C}_2\text{H}_2$ ), benzene ( $\text{C}_6\text{H}_6$ ), ethanal ( $\text{CH}_3\text{CH}_2\text{OH}$ ) and cyclohexane ( $\text{C}_6\text{H}_{12}$ ) as a carbon precursor for large area and high-quality by CVD graphene. Secondly, a gas carrier was mostly introduced into this process as  $\text{H}_2/\text{Ar}$  gas that mixture with together. The both Hydrogen ( $\text{H}_2$ ) and argon ( $\text{Ar}$ ) gases were used for growing graphene films during fabricate a process [9-21]. A hydrogen gas acts as a catalyst for methane to be physically adsorbed on surface substrate for graphene growth, etching agent which controls the morphology of graphene during production and leads to crystallization of Cu foil while argon gas ( $\text{Ar}$ ) acts as a carrier

gas that provides an inert ambience [22-25]. In addition, the substrate that properly expected using to synthesis graphene, lowest surface roughness at a non-appeared contaminant as an oxide on surface and the large grain boundary on substrate (111) mechanism crystal orientation. Typically, copper (Cu) foil is usually use to substrate that growing large area monolayer graphene by CVD process due to its can be easily scaled for mass production as an appearance controller upon monolayer graphene and has lattice size nearly with graphene structure as well as Cu foil has low-cost comparing between other material using as substrate [26]. However, a Cu surface has been occurred rolling lines from manufacturing process as a result to impurities and Cu oxides appeared during the storage. These problem produces to the defects in structure and produced multilayer graphene during growth process. So, the Cu foil surface that appropriate to synthesis a large-area and high-quality monolayer graphene was improved by pretreatment process.

Typically, the part of preparation has the prototype process that commonly rinsing Cu foil surface with solvents acetone ( $C_3H_6O$ ), isopropanol alcohol (IPA) and deionized water (DI water), respectively, but there cannot decrease to rolling lines and the impurities as oxides from Cu foil structure. The process next soaking a Cu foil in hydrochloric acid 37% concentration for remove impurities in Cu foil structure and then etching with  $H_3PO_4$  at 40-60% concentration by electropolishing process under constant voltage at 2.5 V of 130- $\mu$ m-thick Cu foil which is appears to be more convenient as a catalyst pretreatment method because of produces minimal contamination and minimal roughness of 0.9 nm [26, 27]. However, Cu foil surface stilled appearing some rolling line on surface and its polycrystalline generated a lot of small grain size over all crystal plane, such as Cu (111), Cu (200), Cu (220) and Cu

(311) surfaces as a result represent defect and difficult synthesis uniform monolayer of graphene usually grow on Cu (111) crystal plane [28].

In this work, the synthesis of graphene film on treat Cu foil as a substrate by direct liquid injection chemical vapor deposition (DLI-CVD) using nitrogen ( $N_2$ ) as a gas carrier, preparing Cu foil substrate by pretreatment processes with electrochemical polishing processes for reducing surface roughness following traditional process but addition a physical process for removing preliminary rolling line. Finally, the substrate was thermally annealed with nitrogen gas by annealing process for recrystallized structure and grain size that all of process have investigated by optical microscope (OM) as a surface morphology of Cu foil substrate. After that, the substrate moves to graphene growth process using cyclohexane as a carbon precursor under  $N_2$  ambient following the fixed condition such as annealing temperature and growth temperature at the most suitable growth process for graphene film which is investigates the intensity ratio between 2D to G and D to G by Raman spectroscopy (RM).

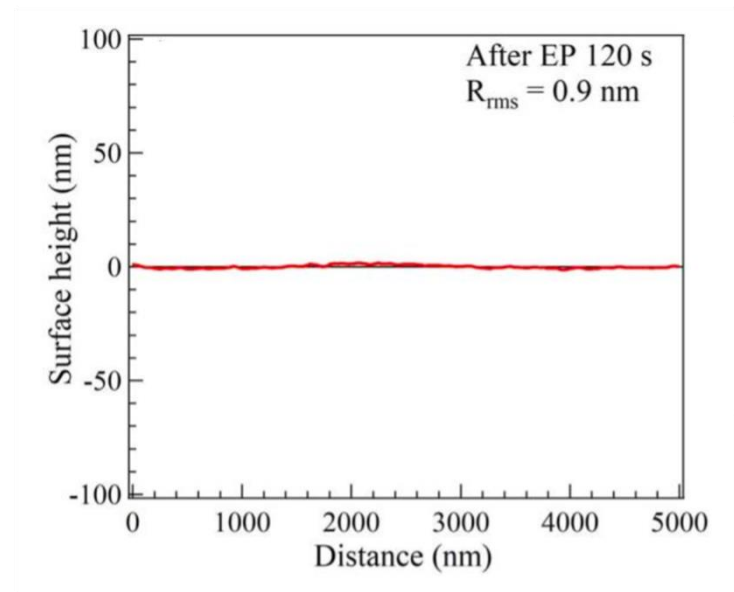


**Figure 1** Surface height of Cu foil after 120 s of electropolishing in a 50%  $\text{H}_3\text{PO}_4$  solution, with an RMS roughness of 0.9 nm. [26]

## 1.2 Overview

The purpose of this work is to studying to structural and a basic understanding of CVD growth process of graphene film on treat Cu foil substrate. The following topics are mainly focus.

1. To study graphene growth on treated and untreated Cu foil substrate with pretreatment process.
2. To characterize structural property of graphene film was grown by CVD method.

## 1.3 Expectation

The high quality of graphene films was successfully grown on treat Cu substrate foil with pretreatment processes by CVD process with  $\text{N}_2$  carrier gas using cyclohexane as a liquid carbon precursor.

## 1.4 Organization of the thesis

The organized of this thesis is following by:



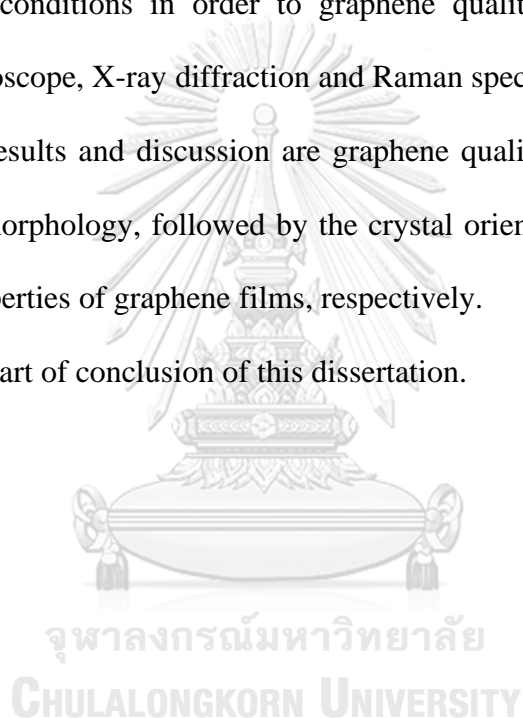
**In Chapter I**, overview, and motivation of graphene growth which the DLI-CVD process to used produce a graphene were explained.

**In Chapter II**, the background of a graphene is explained which inclusive of physical properties, substrate preparation and growth process, and characterization methods.

**In Chapter III**, experimental details, including substrate preparation, DLI-CVD growth and structural measurements are explained in terms optimization of Cu foil substrate surface conditions in order to graphene quality by optical microscope, atomic force microscope, X-ray diffraction and Raman spectroscopy.

**In Chapter IV**, results and discussion are graphene quality by optimized preparing process, surface morphology, followed by the crystal orientation of Cu foil substrate and structural properties of graphene films, respectively.

**In Chapter V**, a part of conclusion of this dissertation.



## CHAPTER II

### BACKGROUND AND TREORY

#### 2.1 Structural and property of graphene

##### 2.1.1 Structural property

The carbon is a group four elements in table that it is normally fabricate many compound and crystalline of solid. The graphene is a monolayer of carbon atoms while graphite is multilayer of carbon atoms as six atoms of carbon, as shown in Figure 2. In orbitals on the ground state such as  $1s^2$ ,  $2s^2$ ,  $2p_x$  and  $2p_y$  orbitals that electrons have been filled in the  $1s$  orbital pattern to the core shell while the two paired electrons and two unpaired electrons in the  $2s$  and  $2p$  orbitals which one electron in  $2s$  orbital is stimulated to the  $2p$  orbital, then four unpaired electrons are generated in the  $2s$ ,  $2p_x$ ,  $2p_y$  and  $2p_z$  orbitals result to  $2s$ ,  $2p_x$ ,  $2p_y$  orbitals have been coordinated as a  $sp^2$  hybridization structure [29]. The  $sp^2$  hybridized orbitals are very strong structure in the graphene crystal refer to  $\sigma$  bond as an individual carbon atom which is placed in a graphene lattice by covalent bonding with three of its closest neighbor atoms. On the other hand, an un-hybridized orbitals of valence electron in the  $2p_z$  were formed by Van der Waals bonding refer to  $\pi$  bond as an each holding between graphene layers and hybridized orbitals are arranged in a triangle with an angle of  $120^\circ$  between the bonds, as following in Figure 3.

##### 2.1.2 Crystal structure

The structure of graphene film is 2D structural which has been hexagonal in honeycomb crystal. Graphene has lattice parameter ( $a_0$ ) about  $1.42 \text{ \AA}$  neighbor atom and the opposites atom bonding which its vectors  $a_1$  and  $a_2$  have the same lattice constant ( $a$ ) of  $2.46 \text{ \AA}$  as a primitive unit vector, can be defined following.

$$\vec{a}_1 = \frac{\sqrt{3}a}{2}, \frac{a}{2} \text{ and } \vec{a}_2 = \frac{\sqrt{3}a}{2}, -\frac{a}{2}$$

Where  $a = \sqrt{3}a_0 \approx \sqrt{3} \times 1.42 = 2.46 \text{ \AA}$  is vectors  $a_1$  and  $a_2$  refer to lattice constant that is the distance between unit cells. The position vector of the  $B_1$ ,  $B_2$ ,  $B_3$  atoms relative to the A atom is expressed as  $\vec{R}_1$ ,  $\vec{R}_2$ , and  $\vec{R}_3$ , as shown in Figure 4a) and the three atoms nearest neighbor vectors are given by

$$\vec{R}_1 = \left( \frac{a}{\sqrt{3}}, 0 \right), \quad \vec{R}_2 = \left( -\frac{a}{2\sqrt{3}}, -\frac{a}{2} \right) \text{ and } \vec{R}_3 = \left( -\frac{a}{2\sqrt{3}}, \frac{a}{2} \right)$$

$$\text{Where } |\vec{R}_1| = |\vec{R}_2| = |\vec{R}_3| = a_0$$

A Figure 2b refer to the reciprocal lattice of hexagonal graphene structure. It be seen that the reciprocal lattice vectors  $b_i$  is defined as a function of the primitive lattice vector  $a_i$

$$b_1 = 2\pi \frac{a_2 \times a_3}{a_1 \cdot a_3 \times a_3}, b_2 = 2\pi \frac{a_3 \times a_1}{a_2 \cdot a_3 \times a_1} \text{ and } b_3 = 2\pi \frac{a_1 \times a_2}{a_3 \cdot a_1 \times a_2}$$

$$\text{Where } b_1 = \left( \frac{2\pi}{\sqrt{3}a}, \frac{2\pi}{a} \right) \text{ and } b_2 = \left( \frac{2\pi}{\sqrt{3}a}, -\frac{2\pi}{a} \right); |\vec{b}_1| = |\vec{b}_2| = 4\pi/\sqrt{3}a.$$

Due to crystal structure of graphene is 2-dimensional structure result to it does not has appeared to  $b_3$  in reciprocal lattice which both of formulars are explain an electronic band property of graphene, as shown in Figure 4b). The Brillouin zone was used to describe dispersion relation of graphene that has been created with representative a line that intersects the core from nearest neighbor atoms and the line was intercepted with perpendicular as a defines the shaded area. There are three key positions identified by  $\Gamma$ -point,  $M$ - point, and  $K$ -point. The center of a Brillouin zone is  $\Gamma$ -point[30], in contrast  $M$ - point and  $K$ -point were described with  $IM$  and  $IK$  vector to comparing respect to the  $\Gamma$ -point, as following by.

$$\Gamma M = \left( \frac{2\pi}{\sqrt{3}a}, 0 \right) \text{ and } \Gamma K = \left( \frac{2\pi}{\sqrt{3}a}, \frac{2\pi}{3a} \right)$$

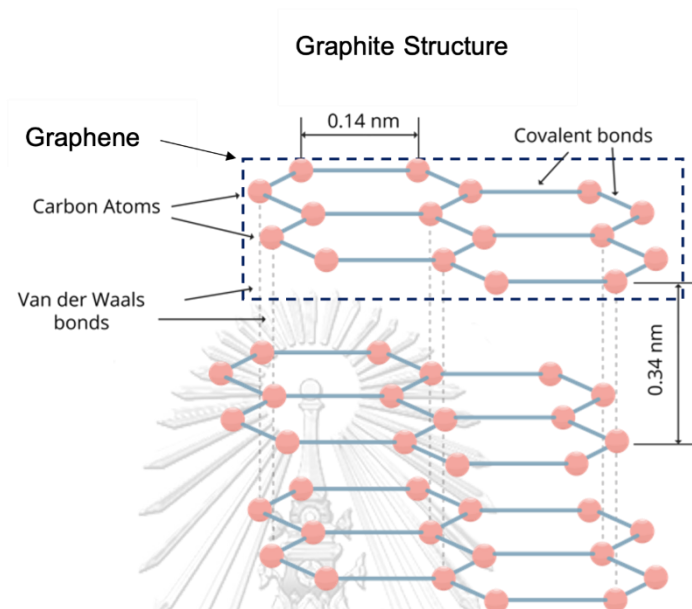


**Figure 2** Structural differences between graphite and graphene.

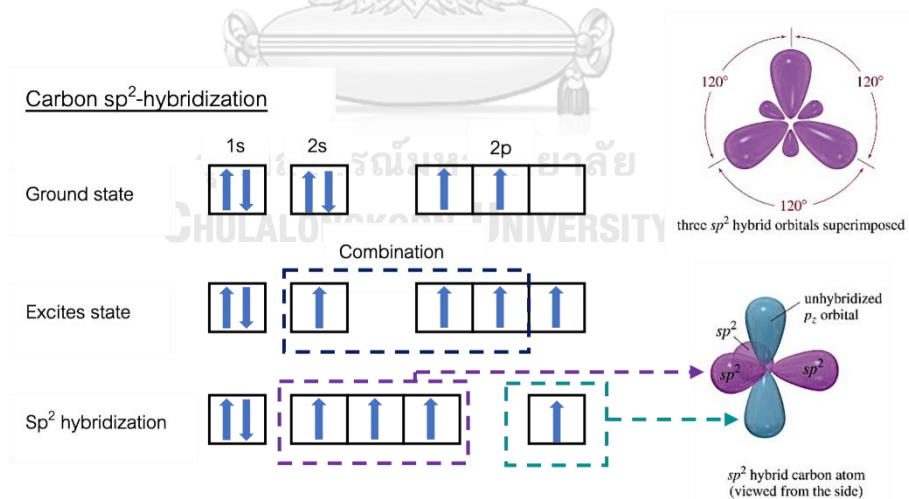


**Figure 3** Carbon diagram depicting  $sp^2$  hybridization, adapted from. [29]

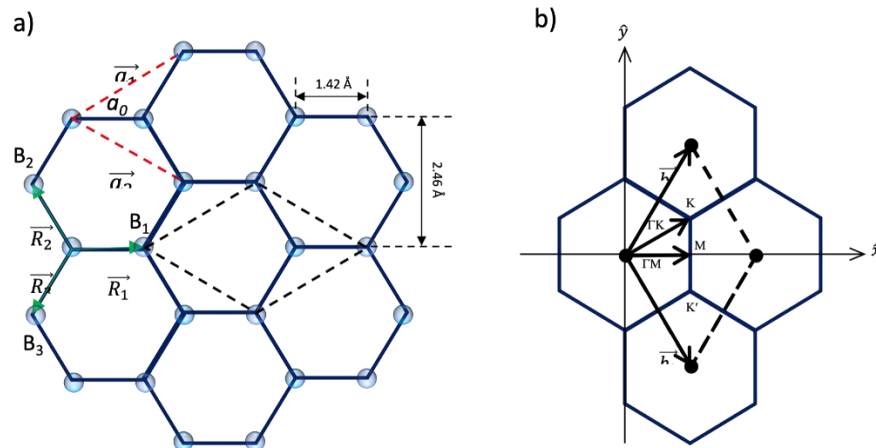


**Figure 4** Schematic representation of the graphene lattice, and b) reciprocal lattice of the graphene lattice.

### 2.1.2 Electrical property

Graphene energy band structure using the six nearest neighbor atoms in reciprocal space at points K and K', the dispersion relation was determined by two pairs according to K to Gamma, one by  $\Gamma$  to M and three by M to K. In this model, Fermi energy was found at the point whereas the conduction and valence bands touch at point K refer to Dirac point, as following in Figure 5.

$$E_{2D}^{\pm}(k_x, k_y) = \pm t_0 \sqrt{1 + 4 \cos \frac{\sqrt{3} k_x a}{2} \cos \frac{k_y a}{2} + 4 \cos^2 \frac{k_y a}{2}}$$

Where used to calculate the band 2D structure of graphene.

The maximum value of the valence band and the minimum of the conduction band degenerate at point K, resulting in a zero-energy band gap because of the corresponding points in the plane, the material is straight, especially that the energy dissipation around point K is linear, which corresponds to the relativistic Dirac point distribution. The active valence and empty conduction bands met at the zero-state density (DOS) Dirac point because of the graphene is represented as a zero-gap

semiconductor with DOS occurring at the Dirac point, so graphene has appeared energy gap between the valence and conduction band. The relativistic Dirac equation is often used with charge carriers (electrons or holes) whereas supposed to massless as a result to Dirac Fermions of electrons and holes travel at a velocity  $v_F \approx 1 \times 10^6$  m/s.

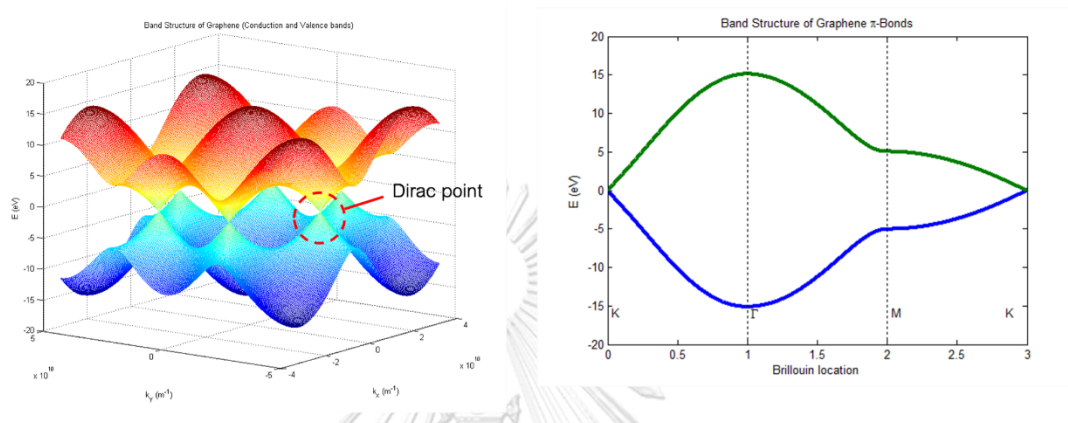


**Figure 5** Band structure of graphene's  $\pi$ -Bond (Conduction and Valence bands). [31]

## 2.2 Substate preparation and graphene growth process

### 2.2.1 Substate preparation

In this work using the Cu foil as a substrate for graphene growth process but Cu foil in commercial has impurities, oxides and (rolling lines or surface roughness) on its surface. In addition, the crystalline orientation of the Cu foil showed a Cu (111) orientation as a result quality of graphene. Therefore, Cu foil surface should be improved to prepare surface for high quality graphene growth. The surface preparation followed by physical polishing, electro-polishing, and annealing process.

#### 2.2.1.1 Electro-chemical polishing

Electro-chemical polishing is an electrochemical process that reduces surface roughness and removes surface contaminated of Cu foil surface part the process leaves a smooth, ultra-clean surface polishing. The Cu foil surface has been dissolved in electrolyte and electro-polishing, acts as a positively charged anode (workpiece)

that connected to the positive pole of the DC power supply; Likewise: negatively charged cathode (Tool cathode) connect to the negative terminal of the DC power supply. Both the anode and cathode were soaked in electrolyte solution such as sulfuric acid and phosphoric acid. The current from the power supply is carried from the anode to the cathode through the electrolyte which bring about the metal ions on the surface of a parts to oxidize and dissolve them into an electrolyte [31] in Figure 6.

The voltage has adjusted to a circuit system, current density and applied voltage following in Figure 7.

Etching state (A to B), the solution of Cu ion transferred,

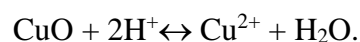


The positive charge gets into Cu plate (cathode) and then electrolyte solution decomposing to Cu atom building Cu foil ion that reaction on surface. In this state is appropriate for electro etching process.

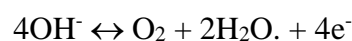
Passivating state (B to C), oxide layer formation,



Polishing state (C to D), this state is constantly chemical reaction (redox reaction) which is suitable for electropolishing.



Pitting state (D to E) oxygen layer, which is occurred from replacing copper atom with oxygen atom to more decomposition.



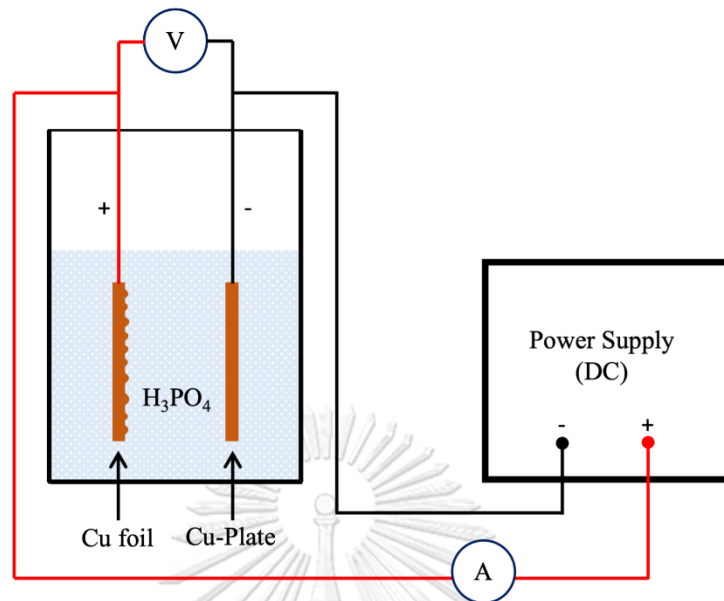


**Figure 6** Schematic representation of the electropolishing process of Cu foil substrate.

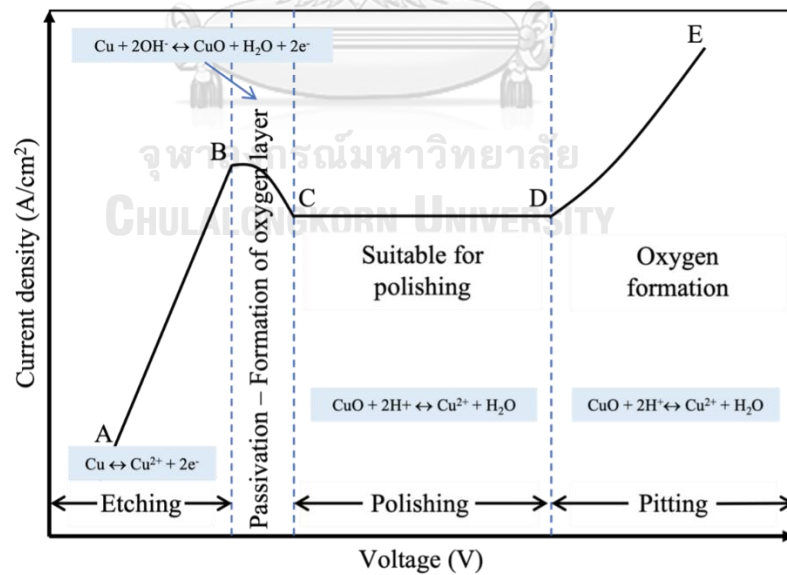


**Figure 7** J-V characteristic of the electropolishing process.



### 2.2.1.2 Annealing process

Thermal annealing heated treatment to Cu foil due to it is polycrystalline structure, for performed to produce a specific microstructure including to eliminate stress, grain size and improve polycrystal structure become to single crystal structure for overall structure homogeneous. The main steps for the annealing process, heating the Cu foil surface to the selected temperature remaining at that temperature, and then cooling to room temperature. A crystallization is one of the expected results in thermally stimulating microstructure evolution processes as a result in stress-free grains occurring from the deformed in structure. Moreover, the new grains increase in size. The characterized can change the crystalline orientation of a grain crystals of the Cu foil before annealing to Cu foil surface shown the desired (200), (022) and (311) directions in contrast, the (111) plane is influenced after annealing process [24, 32-34].

### 2.2.3 Graphene growth process

#### 2.2.3.1 Chemical Vapor Deposition

Chemical Vapor Deposition (CVD) is normally growth of graphene is the most useful in method to preparation monolayer of high-quality graphene structure and purity for use in various devices. Graphene is grown on a substrate can be into two route methods similar with CVD and different in precursors, the distribution of reactive to the surface of catalyst substrates and the catalyst grown of graphene. The stable condition gas flow rate of a composition of reactively gases on the surface of a catalytic, that the gas flow rate dependents on the pressure and chamber length. The fabrication of graphene on a metallic catalyst interlaces several primary steps: 1)  $\text{CH}_4$  is used an agent to the precursors carrier into the CVD reactor; 2) the gases precursors for a reaction to form product ( $\text{C}_x\text{H}_y$ ) in the vapor phase; 3) the carbon is distributed

to the surface to achieve layer on substrate surface; 4) adsorption of the carbon into the surface ( $\text{CH}_x$ ); 5) decomposing of the adsorbed carbon to form produce carbon and distributed on the surface; 6) the product (C-C) forming the graphene lattice; 7) the inactive product (e.g., hydrogen) will desorbing from the surface to producing molecular hydrogen or other products; and 8) the products distributing from the surface to the boundary layer and finally being removed by the gas flow is described in Figure 8.

### 2.2.3.2 Direct Liquid Injection Chemical Vapor Deposition

Direct Liquid Injection Chemical Vapor Deposition (DLI-CVD) is modified from normal CVD by injects a liquid precursor into the chamber to controlling the flow rate and quantity of precursors, and to high quality and less impurity of graphene sheet. The liquid injection head is included a liquid injector, mixture chamber and mixture injector. The liquid injector injects the liquid precursor into the mixing chamber where the liquid and gas are mixed. Finally, the precursor sends to growth process of graphene [35].

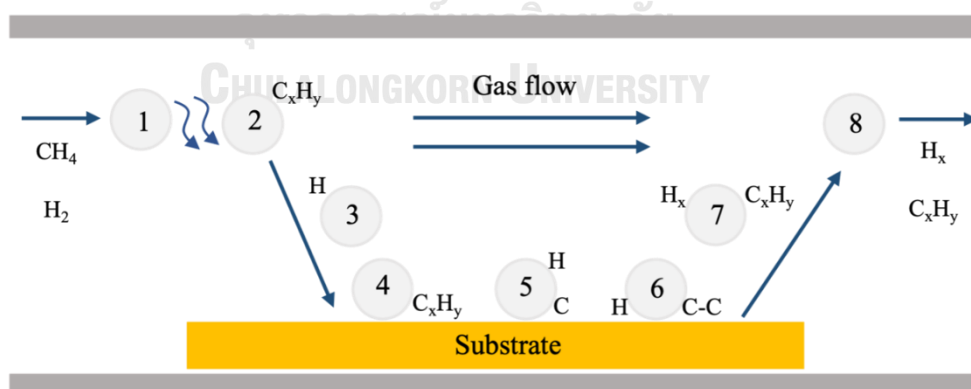


**Figure 8** Growth mechanism of graphene by CVD on metal substrates: Elementary steps for graphene growth on a catalytic substrate.

## 2.3 Characterization of graphene

In this work, characterization methods measured to graphene films. Optical microscope (OM) was measured to investigate surface and morphology of the films. X-ray Diffraction and Raman scattering were characterized for investigating structural properties.

### 2.3.1 Optical microscope

The optical microscope (OM) method is study to the morphological of objects, which is used to various laboratories. The novel optical microscopes can magnify objects 1500 times with a limited spatial resolution of 0.2  $\mu\text{m}$ . The optical microscopes can be classified into several categories using a variety of standard, for example, according to the method of lighting. The light beam is generated and output from the light source. After that, the beam will be sent to condenser lens, which serves to combine the light to have the most intensity to shine the object on the substrate slide as bright as possible. when the light is passed to condenser lens, which light beam into the specimen stage. The specimen stage seizes position of the sample and controlling to the left and right to quick image search, and a scale indicates the position of objects on the slide. After a light beam into objective lens, a lens that is closest to the object that enlarges the resulting image. It will have magnification is indicated, e.g., x4, x10, x40 or x100, etc. The result of objective lens sends to eyepiece lens, lens at the top of the optical microscope [36]. In general, there are a magnification of 10x or 15x, which serves to enlarge the image obtained from the objective lens to be larger, causing images that the eye of the study can view.

### 2.3.1 X-ray diffraction.

X-ray diffraction is useful technique that provides detailed information about to lattice parameter and structural properties. The X-ray beam focuses to projection the sample and then diffracted under the atomic to atomic on different planes in the sample. The incident rays interacted with the atom in crystal of sample. After that, X-ray is caused constructive interference (and diffracted rays) by conditions satisfy Bragg's law ( $n\lambda=2d \sin \theta$ ) that relates the wavelength of X-ray radiation to the diffraction angle and the d-spacing in a crystalline sample. The conversing of the diffraction peaks to d-spacings allows identifiable of the sample that each sample has a unique d-spacings and being done by comparing the d-spacing with the standard reference model in Figure 9.

### 2.3.2 Raman spectroscopy

Raman spectroscopy (RM) based on the principle of scattering of light caused by photons hitting molecules of a certain wavelength laser light through a sample. There will be several photons that will pass through them. While some will collide with molecules and change direction. In that collision, for the most part of the energy light after the collision does not change to an elastic collision, known as Rayleigh scattering, but a small fraction of the photons at energies. After that the collision is changed due to the exchange of energy with molecule, also known as inelastic transport, the photon may have a greater or lesser frequency. The change in energy after the collision is called Raman scattering. If photons collide with a molecule in the ground state, the frequency after the collision is reduced, known as stokes Raman scattering, but if the light particles catch with the molecules in the excitation state, the post-collision frequency is increased, known as anti-stokes Raman scattering. In the

general measurement is used Stokes Raman scattering because of higher intensity. Raman spectroscopy can study many aspects of graphene produced, such as the number of graphene layers. The quality of the graphene produced or the effect of surface on graphene. For the presentation to the high quality of graphene film. The graph measurement is plot between the Raman shift ( $\text{cm}^{-1}$ ) and the photons intensity is scattered. The Raman shift is defined by

$$\text{Raman shift} = \frac{1}{\lambda_{\text{incident}}} - \frac{1}{\lambda_{\text{scattered}}}$$

where  $\lambda_{\text{incident}}$  and  $\lambda_{\text{scattered}}$  are the wavelength of the incident and scattered photons, respectively. The value is related to photon energies of bonds in the sample.

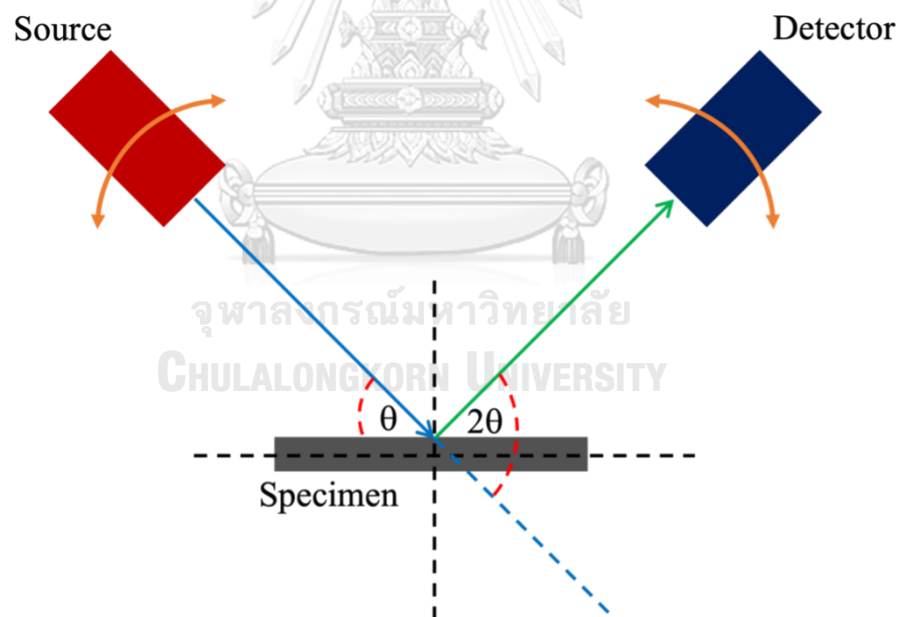


**Figure 9** Schematic illustration of the X-ray diffraction process.

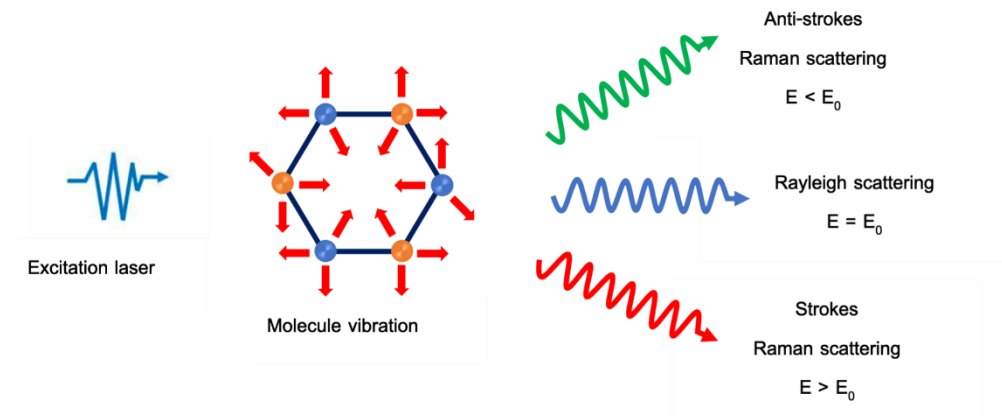


**Figure 10** Schematic of Raman scattering process.

### 2.3.3 Raman band of graphene

Raman is study in atomic type of bonding in structure from the vibration of graphene lattice, different bond used to different energy of lattice vibrations specify to type of substance. By the way, for graphene-based applications, according to investigates, which the key to separating the quantity of graphene sheets and the impact quantity of the defectively on properties. The Raman spectroscopy is appropriate and relies on the process of verifying both properties. The high-spectra resolution of Raman spectroscopy coordinated with the advanced structure selectively and non-hazardous nature of this process make it a standardized equipment in the field of graphene rapid growth. The G-band characterizes most of the graphene and is shown to be  $1580\text{ cm}^{-1}$  [37-39]. This is highly susceptible to strain and an effective quantitative indication on graphene plates. The position of the G band transfers to the low frequency as the number of sheets increases as shown in Figure 11. Maybe, not important changing has been found of spectra appearance. Moreover, the G-band is sensitive to doped, the peak amplitude and the frequency of this peak maybe apply to measure the doping range. The D band can be called the deformation band, occurs

from structure motional distancing to the center of Brillouin zone and during like 1270 and 1450  $\text{cm}^{-1}$ . The 2D band is a two-time phonon system, a high frequency dependent on the stimulation wave due to the dual resonance procedure, that connects the photon wave vector to the electronic loop structure. This peak occurs at about 2700  $\text{cm}^{-1}$ , as shown in Figure 11. However, the behavior of 2D is more than complex compared to the frequency shift seen for the G-band.

A previous section mentions to D and 2D peak when the direction of the zone-center mode is parallel (or perpendicular) between the carbon (C-C) atom bonds which are called transverse (T) and longitudinal (L) phonon modes. The phonon distribution relationship in Raman mode in graphene that it has six phonon type with two atoms per unit cell. There are three phonon acoustic (A) modes and three optical (O) modes. The four phonon modes are called in-plane vibrating modes, which have two acoustic modes and two optical modes. The other two phonon modes are out-of-plane vibrating modes.

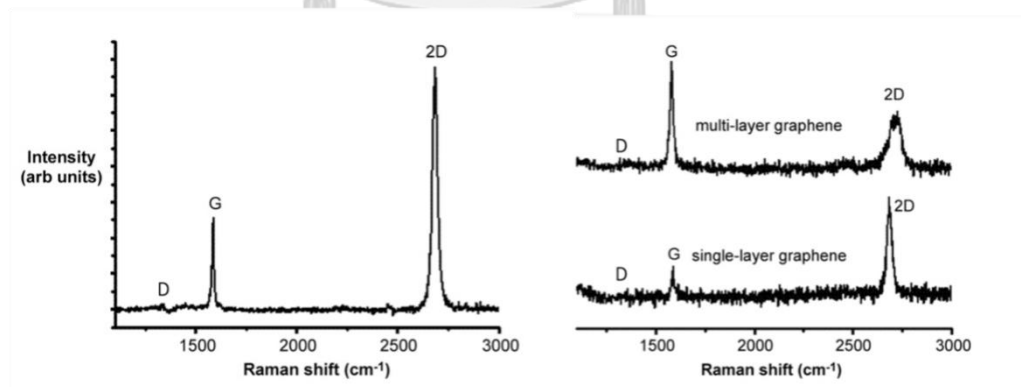


**Figure 11** Positions of D, G, and 2D bands in the Raman shift of graphene structure

### G band

G band is phonon vibrations of TO and LO phonon scattering modes which is the first order to Raman band in graphene structure, including with the incident phonon as an electron or hole that the resonantly excites for translation on conduction band and drop to valence band. There is characterized by scattering individual TO or LO at the core-zone ( $\Gamma$ ) phonons. The excited electron-hole pairs are then recombined and emitted energy photons, as shown in Figure 12.

### D band

The D-band occurs near  $1350\text{ cm}^{-1}$ , relate with TO photon around the K-point refer to disorder structure. On the other hand, G band or 2D band, D band is required to conserve the momentum of the defect. Raman scattering process consists of inelastic electron scattering by TO photons to K-point and inelastic back scattering to k-point due to defects. The energy change for the D band was found to be half of the 2D band.

### 2D band

A 2D band peak is a graphene as a called double resonant (DR), highest intensity which is a process caused by the vibrational mode in the carbon ring plane. The in-plane vibration mode for the carbon ring while the 2D process diagram excites Raman. Electron-hole pairs are created by incident photons near K-point, inelastic scattering of electrons by TO photons to K-point for reasons of conservation of energy and momentum in the Raman process.



### D' and 2D' band

This creates a point called D' peak, which is visible approximately  $1620\text{ cm}^{-1}$  in the defected graphite. 2D peak' is the double resonance of peak D' occurring from a Raman scattering process in which the conservation of momentum which is achieved by the participation of two electrons with opposite vectors ( $q$  and  $-q$ ), thus always present and they do not require defects for their activation [38, 40].

To examined number layer of graphene films that the parameter obtained from the Raman spectral analysis of graphene is the 2D-to-G-band as a Raman intensity ratio ( $I_{2D}/I_G$ ). Parameters consisting of the  $I_{2D}/I_G$  ratio that the full width of half maximum (FWHM) of both peaks were used to characterize the number of layers of graphene [41]. The Raman intensity approximately twice of the 2D bands compared to the G bands, the graphene sheets are confirmed to be single layers. Moreover, the appearance of D-peak as a determined of defects in graphene layers. All parameters obtained from the Raman spectra of graphene were summarized. In addition, the relationship between the Raman spectral information and the Raman laser excitation wavelength was summarized. as well as the number of layers of graphene [28, 34, 42, 43].

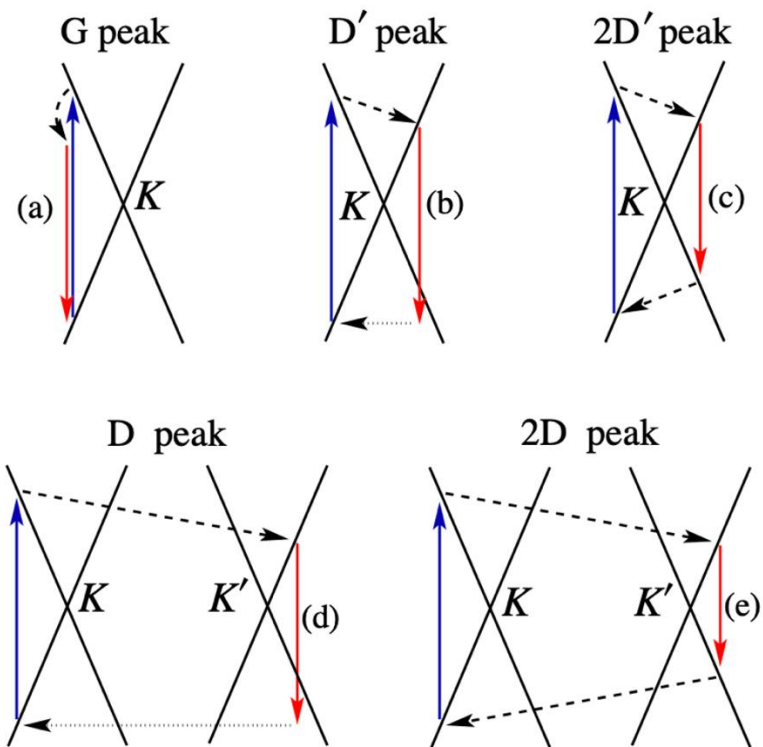


**Figure 12** Schematic illustration of the translational process of D, G, and 2D bands, adapted from [34]

## CHAPTER III

### EXPERIMENTAL DETIALS

This work focuses on investigating the surface preparation of Cu foil to synthesize graphene films using the CVD process. The Cu foil, with a thickness of 25  $\mu\text{m}$ , is cut into 4 x 5  $\text{cm}^2$  pieces, and two sets of experimental processes are conducted. The first surface preparation process involves cleaning the Cu foil with acetone, followed by rinsing with isopropanol alcohol (IPA), DI water, and then etching with electropolishing in phosphoric acid. The second set includes physical polishing (PP) with Brasso, followed by cleaning with acetone, rinsing with isopropanol alcohol (IPA), DI water, and then etching with electropolishing in phosphoric acid, isopropanol alcohol, and DI water. Afterward, the samples are dried using nitrogen gas.

Finally, the prepared samples are subjected to thermal annealing under  $\text{N}_2$  carrier gas to facilitate the subsequent graphene growth process.

### **3.1 Optimization the copper foil surface for graphene growth**

#### **3.1.1 Electro-polishing process**

The electropolishing (EP) processes are aimed at reducing the surface roughness and removing surface contaminants from the Cu foil. Initially, the Cu foil is smoothed at room temperature and subjected to a suitable voltage (2.5 V) for the EP process, utilizing different concentrations of phosphoric acid. The electropolishing time is adjusted to 60, 90, and 120 seconds, while the aqueous electrolyte contains 40%, 50%, and 60% phosphoric acid. The treated samples are then cleaned with DI water and dried with nitrogen gas (as depicted in Figure 13 and 14).

Considering that the Cu foil thickness was changed from Cu-130- $\mu\text{m}$ -thick in previous research to Cu-25- $\mu\text{m}$ -thick for this study, we have chosen to use 30% phosphoric acid. This decision is based on the belief that higher concentration results in a greater quantity of ions, leading to a more pronounced reaction on the Cu foil surface.

To determine the appropriate parameters for the electropolishing process on the smoothed Cu foil substrate, we followed the prototype used in our laboratory, which demonstrated the lowest roughness at 0.9 nm [26]. Hence, we have carefully selected the voltage, time, and percentage for the experiment, aiming to achieve optimal results.

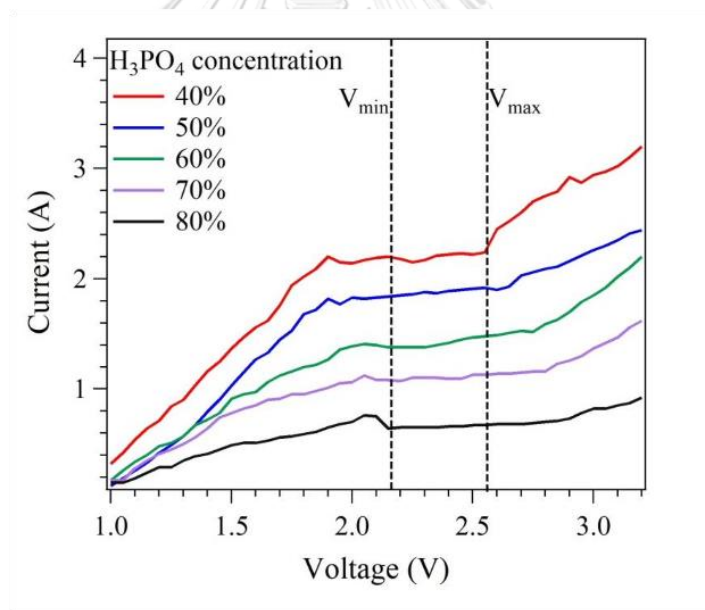


**Figure 13** I-V performance for the electropolishing process at different concentrations of H<sub>3</sub>PO<sub>4</sub>. [26]

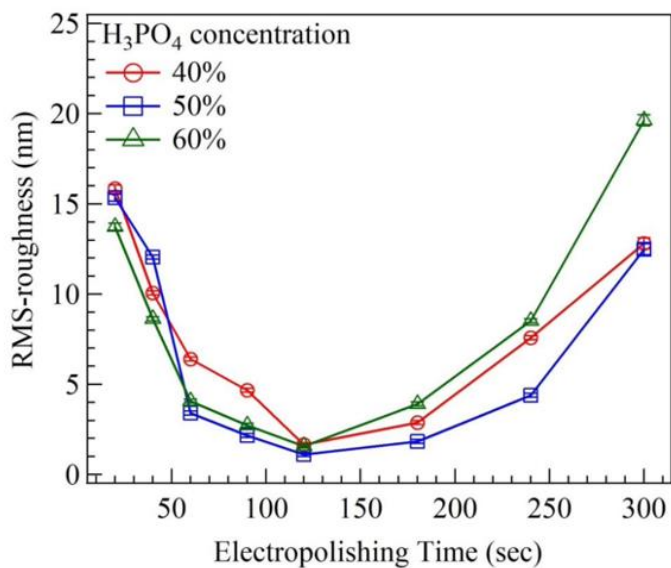


**Figure 14** Optimization of RMS surface roughness of Cu foil at 40%, 50%, and 60% H<sub>3</sub>PO<sub>4</sub> concentrations. [26]

### 3.1.2 Annealing process

Following the pretreatment processes, the treated Cu foil was placed into the chamber and heated using a furnace from room temperature to an annealing temperature within the range of 860-940 °C. The temperature ramp rate was approximately 5 °C/s, and the annealing time was adjusted to 30 minutes.

During the annealing process, N<sub>2</sub> gas was used as the carrier gas at a flow rate of 300 standard cubic centimeters per minute (sccm), maintaining a total pressure of 2 mbar for 10 minutes. Raman spectra analysis showed an increase in the I<sub>2D</sub>/I<sub>G</sub> ratio of about 3 and an I<sub>D</sub>/I<sub>G</sub> ratio of about 0.11, indicating the prevalence of monolayer graphene with low defects. However, some regions exhibited smaller ratios, suggesting the presence of bilayer or multilayer graphene. Further annealing of the Cu foil for more than 10 minutes resulted in graphene with lower I<sub>2D</sub>/I<sub>G</sub> ratios ranging

from 1.0 to 3.0 and  $I_D/I_G$  ratios of approximately 0.2 to 0.4. These observations pointed to the formation of bilayer or multilayer graphene with higher defect levels.

As a result, the copper foils underwent XRD characterization to optimize the annealing conditions further.

### 3.1.3 Graphene growth process

After the proper treatment processes of the Cu foil to facilitate graphene film growth, the next step involves heating the substrate to a constant temperature of 920 °C. The liquid precursor, cyclohexane ( $C_6H_{12}$ ), is introduced into the CVD chamber, with its flow rate controlled at 0.1-0.5 g/min and a duration of 1-10 minutes.  $N_2$  carrier gas flows at a rate of 300 sccm under a pressure of 2 mbar.

The precursor solution is stored at room temperature and pressurized using  $N_2$  to approximately 3.5 bar in the injection head. The  $N_2$  gas carrier mixes with the precursor, causing it to evaporate into tiny droplets, which are then introduced into the vaporizer chamber and heated to 120 °C. The resulting vapor, carried by  $N_2$ , flows into the reaction chamber.

To assess the influence of the pretreatment processes on graphene quality, the study is divided into three parts: physical polishing, electropolishing, and annealing processes. These parts are optimized under the same growth conditions to ensure accurate comparison and evaluation of the graphene's properties.

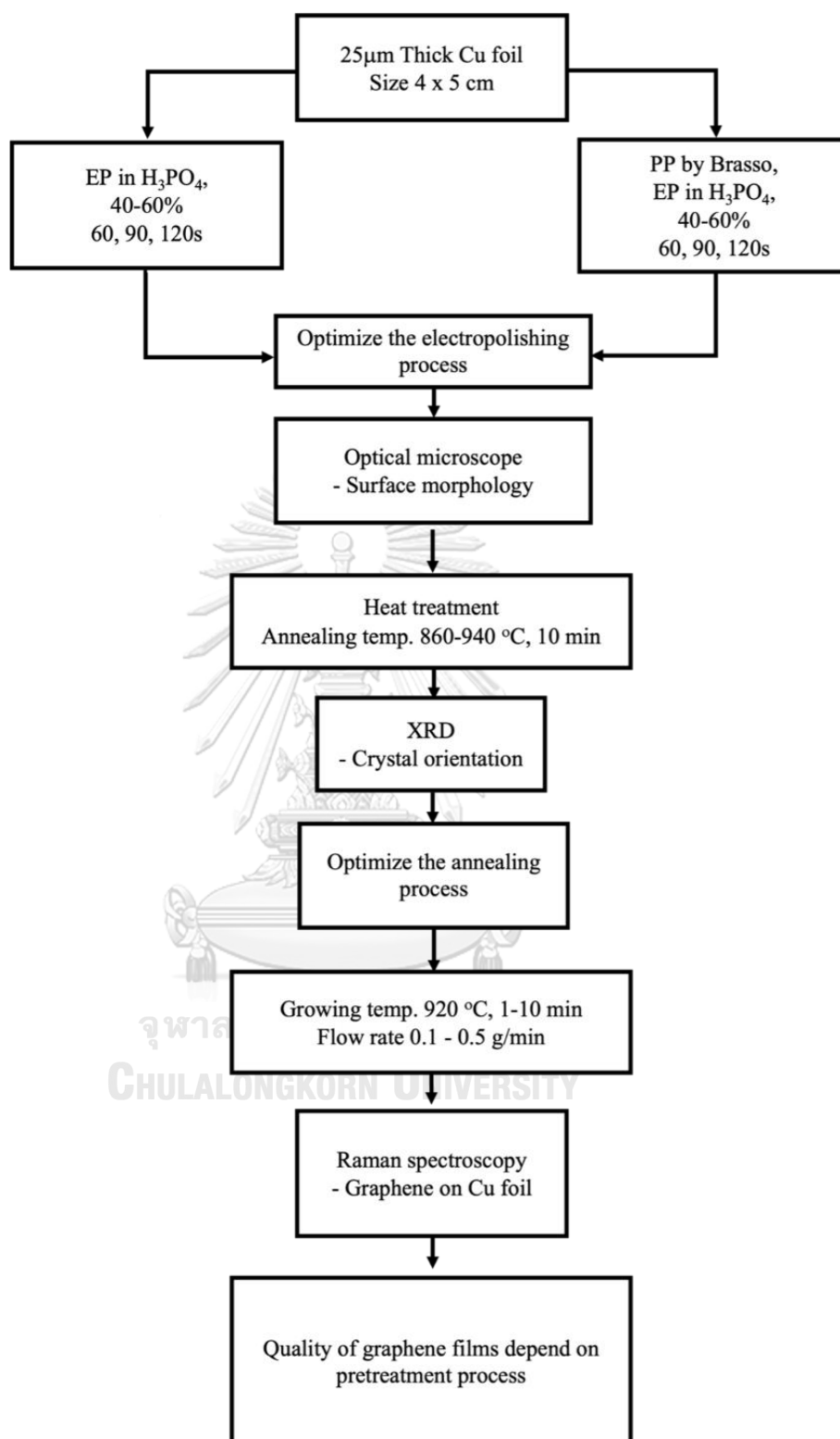


**Figure 15** Flowchart of the experiment illustrating pretreatment and growth process.

### 3.2 Growth of graphene by DLI-CVD method by cyclohexane precursor in N<sub>2</sub> gas carrier

#### 3.2.1 DLI-CVD growth process

After optimizing the conditions for surface treatment of the Cu foil, the growth process focused on finding the optimal annealing temperature for superior graphene quality. The growth temperature, growth time, and flow rate of the cyclohexane precursor were kept fixed during this study. The specific parameters utilized for DLI-CVD graphene growth are presented in Table 1.

Table 1 Parameters of graphene growth by DLI-CVD

Parameters	values
Working pressure	2 mbar
Growth temperature	920 °C
growing time	1-10 min
Annealing time	10 min
Annealing temperature	860-940 °C
Cyclohexane flow rate	0.1-0.5 g/min
Injection head opening time	1ms
Solution frequency	0.5 Hz
N <sub>2</sub> carrier gas flow	300 sccm



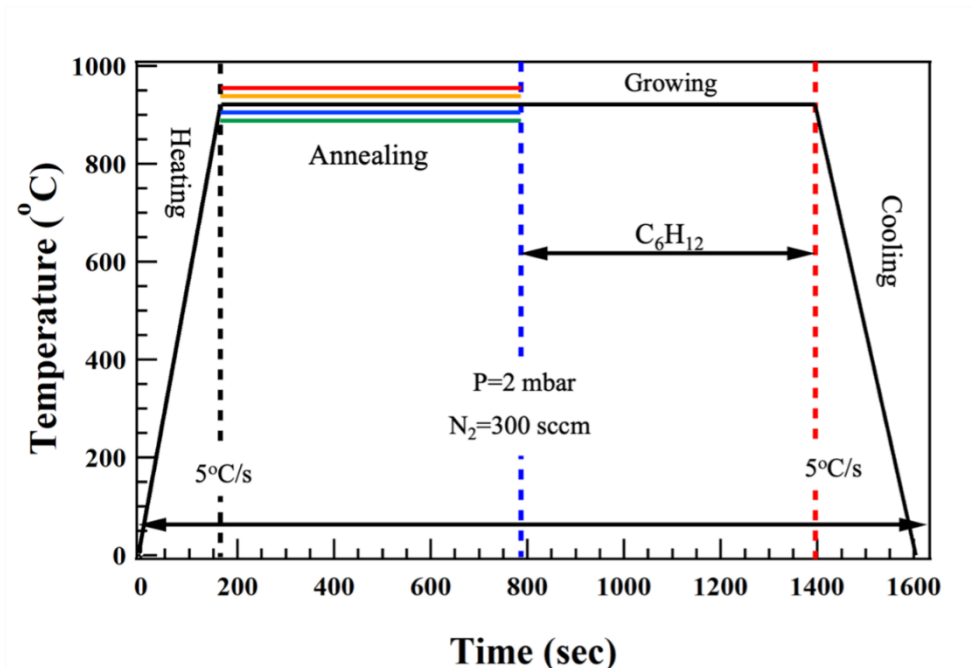


**Figure 16** Profile of the growth process.

### 3.2.2 Characterization Methods

This work employed two distinct characterization methods: one focused on the morphology of the treated copper foil substrate, and the other on the structural properties of the graphene films.

i.) To optimize each process, physical polishing, electropolishing, and annealing were systematically applied, and their effects were evaluated using optical microscopy to study surface morphology and X-ray diffraction to determine the orientation of the treated Cu foil substrate.

ii.) For the structural properties of the graphene films, investigations were conducted using optical microscopy and Raman spectroscopy techniques.

## **CHAPTER IV**

### **RESULTS AND DISCUSSIONS**

In this chapter, we will discuss the characterization of graphene films on Cu foil substrates, utilizing various measurements as mentioned in the previous chapter. The structural properties of the graphene films are closely linked to the conditions of the pretreatment processes applied to the Cu foil substrate for the graphene growth process.

#### **4.1 Optimization of pretreatment processes for graphene synthesis**

The goal of this study is to optimize the Cu foil surface for the graphene growth process using physical polishing, electropolishing, and thermal annealing techniques. The objective is to create a highly suitable substrate that promotes the fabrication of uniform monolayer graphene through DLI-CVD with a cyclohexane carbon precursor under  $N_2$  carrier gas.

In the first process, oxides, impurities, and rolling lines are removed from the substrate. The subsequent steps aim to reduce the surface roughness of the Cu foil and achieve larger grain sizes with a preferred crystal orientation of Cu (111).

Ultimately, by employing various substrate preparation processes, the study aims to enhance the conditions for successful graphene growth.

Figure 17 illustrates the surface morphology of the pre-treated Cu foil, which is 25- $\mu\text{m}$ -thick. This representation highlights the presence of rolling line frequency, surface contamination, and oxide on the surface. To address these issues, a physical polishing technique using Brasso is applied to eliminate these imperfections.

Subsequently, acetone ( $\text{C}_3\text{H}_6\text{O}$ ) is employed as a cleaning agent for the Cu foil surface. Its effectiveness lies in its ability to dissolve grease, wax, and other contaminants and impurities left after the physical polishing process. The final step involves etching the surface using an electropolishing process, which can also be referred to as a polishing method.

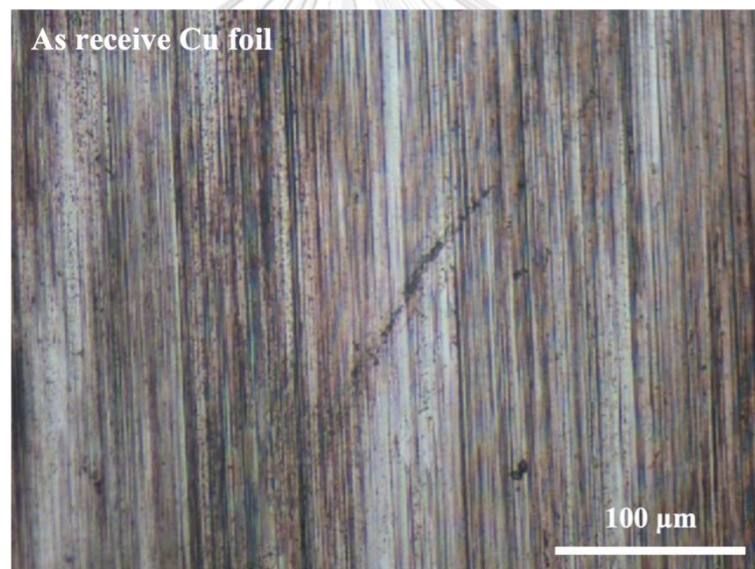


**Figure 17** Optical image of the untreated Cu foil surface.

#### **4.1.1 The effects of treatment process to Cu foil surface**

To achieve a smooth surface on the Cu foils for the graphene growth process, various polishing methods were employed. Electropolishing (EP) was performed using different concentrations of phosphoric acid ( $\text{H}_3\text{PO}_4$ ) ranging from 30% to 60%, with a dipping time of 90 seconds, aiming to optimize the surface roughness of the Cu

foils. Figure 18 shows optical images illustrating the surface of the Cu foils after the EP treatment (without physical polishing by Brasso solvent).

Cu foils subjected to EP with 30% and 40%  $\text{H}_3\text{PO}_4$  concentrations exhibited a rough surface with small grain sizes. However, the Cu foils treated with a 30%  $\text{H}_3\text{PO}_4$  concentration displayed larger grain sizes and higher surface roughness compared to those treated with a 40%  $\text{H}_3\text{PO}_4$  concentration.

Conversely, The Cu foil treated with the 60%  $\text{H}_3\text{PO}_4$  concentration shows some contrast, indicating surface damage due to the high concentration of  $\text{H}_3\text{PO}_4$ . However, Cu foils treated with 50%  $\text{H}_3\text{PO}_4$  concentrations showed minimal surface roughness, with only slight residual line scratches from the Cu foil fabrication process. Among the EP processes using different  $\text{H}_3\text{PO}_4$  concentrations, the Cu foil treated with a 50%  $\text{H}_3\text{PO}_4$  concentration exhibited the smoothest surface.

To achieve fine-tuned surface roughness for our experiments, an  $\text{H}_3\text{PO}_4$  concentration in the range of 45% to 55% was found to be ideal. However, it is crucial to be mindful of the Cu foil thickness when using high  $\text{H}_3\text{PO}_4$  concentrations for EP. Instances were observed where using a 60%  $\text{H}_3\text{PO}_4$  concentration for a dipping time of 90 seconds led to Cu foil breakage after the EP process. Therefore, careful consideration is necessary when selecting the appropriate  $\text{H}_3\text{PO}_4$  concentration to strike a balance between surface roughness and foil integrity.

Additionally, it's important to note that the EP process alone may not completely eliminate all rolling lines from the surface of the Cu foils. Consequently, further optimization of the polishing process is required to achieve truly smooth Cu foils for effective graphene growth. This is essential since the surface roughness of the

Cu foils significantly impacts the quality and properties of the resulting graphene films.

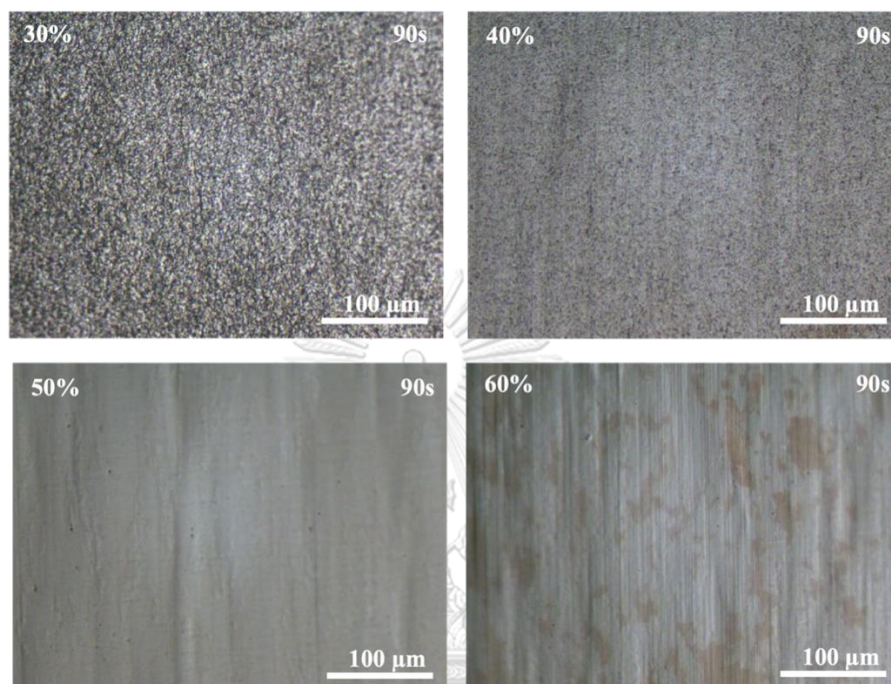


**Figure 18** Optical images of Cu foils after electropolishing with varying concentrations of phosphoric acid ( $H_3PO_4$ ) (30%, 40%, 50%, and 60%) for 90 seconds.

To achieve smoother Cu foil surfaces, a physical polishing process using Brasso solvent was employed before the EP process. The EP process was then fine-tuned, utilizing  $H_3PO_4$  concentrations of 45% and 50%, and varying dipping times of 60, 90, and 120 seconds.

Figure 19 displays optical images of Cu foils obtained from the EP process with a 45%  $H_3PO_4$  concentration, comparing the results with and without physical polishing using Brasso solvent after EP. The findings revealed that pre-polishing the Cu foils with Brasso solvent before the EP process led to smoother surfaces for all

dipping times. Particularly, with a dipping time of 90 seconds, the surface rolling lines appeared on the Cu foils significantly decreased.

However, caution must be exercised with a dipping time of 120 seconds, as it may lead to excessive etching, potentially damaging the Cu foil. Furthermore, when pre-polished Cu foils were subjected to the EP process with a 50%  $\text{H}_3\text{PO}_4$  concentration, a further reduction in surface rolling lines was observed, but the Cu foils exhibited a thinner thickness.

The results indicate that Cu foils subjected to pre-polishing and the EP process with a 45%  $\text{H}_3\text{PO}_4$  concentration for a dipping time of 90 seconds were identified as the optimal substrate for graphene growth in this study.

The integration of pre-polishing and EP processes led to enhanced surface smoothness, a critical factor in facilitating the growth of high-quality graphene films on Cu foils. These findings underscore the importance of meticulous substrate preparation to achieve desirable surface characteristics, ultimately enhancing the quality and properties of the resultant graphene films.

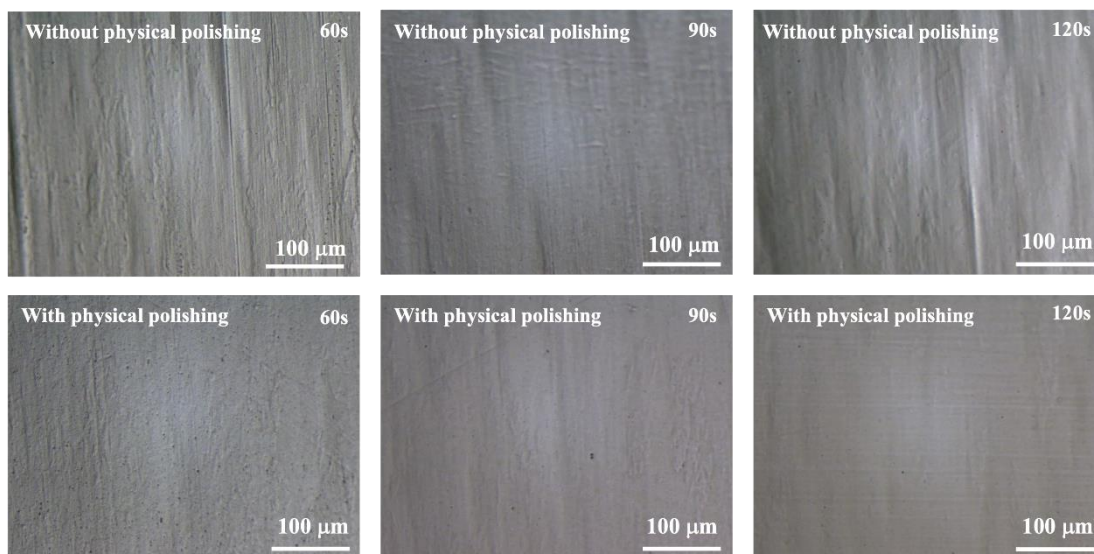


**Figure 19** Optical images of Cu foils obtained from the electropolishing (EP) process with 45%  $\text{H}_3\text{PO}_4$  concentration, comparing the results with and without Brasso polishing after EP, depicting different dipping times of 60, 90, and 120 seconds.

#### 4.1.2 The thermal annealing process effects.

##### 4.1.2.1 Structural properties of Cu foil surface by heat treatment.

Annealing the Cu foil at temperatures ranging from 860 to 940 °C in a  $\text{N}_2$  atmosphere for 10 minutes revealed XRD diffraction peaks corresponding to Cu(111), Cu(200), Cu(220), and Cu(311), indicating a polycrystalline structure. The highest intensity of the Cu(111) peak was observed at 860 and 940 °C, as shown in Figure 20a. After the growth of graphene, the same five diffraction peaks remained present, indicating a consistent Cu(111) orientation at 880, 920, and 940 °C. Additionally, at 920 °C, a Cu(222) orientation was obtained, suggesting a large number of (111) Cu plane. This indicates that the annealing temperature of 920 °C may be optimized for producing monolayer graphene, as shown in Figure 20b.

#### 4.1.2.1 The effect of annealing process on graphene growth process.

The impact of the annealing process on graphene films grown using DLI-CVD in a N<sub>2</sub> atmosphere with a cyclohexane flow rate of 0.5 g/min and a constant growth temperature of 920 °C for 6 minutes was investigated. The annealing temperature was varied from 860 to 940 °C for a duration of 10 minutes. Raman spectra were obtained for the graphene samples immediately after copper foil annealing, revealing different intensities of the D and 2D bands with increasing annealing temperatures. Figure 21a shows the behavior of the I<sub>2D</sub>/I<sub>G</sub> intensity ratio as a function of the substrate annealing conditions.

Graphene films grown on treated Cu foils displayed characteristic peaks at positions of approximately 1358 cm<sup>-1</sup>, 1585 cm<sup>-1</sup>, and 2700 cm<sup>-1</sup> for the D, G, and 2D bands, respectively. The intensities of these peaks varied with different annealing temperatures. Figure 21b illustrates the intensity ratios of I<sub>2D</sub>/I<sub>G</sub> and I<sub>D</sub>/I<sub>G</sub> for graphene films grown on Cu foils at a growth temperature of 920 °C for 6 minutes, with annealing temperatures ranging from 860°C to 940°C. The annealing time was fixed at 10 minutes. Within the annealing temperature range of 880°C to 900 °C, the I<sub>2D</sub>/I<sub>G</sub> intensity ratio exceeded ~2.0, indicating the presence of monolayer graphene films. At other annealing temperatures, the intensity ratio of I<sub>2D</sub>/I<sub>G</sub> suggested the formation of graphene with few or multiple layers. However, the intensity ratio of I<sub>D</sub>/I<sub>G</sub>, which remained below 1.0, was not significantly influenced by the annealing temperature prior to graphene growth. This may be attributed to defect formation or disorder during the nucleation of graphene.



The annealing temperature is crucial in controlling the preparation of Cu foil surfaces for the growth of monolayer graphene films using DLI-CVD. At annealing temperatures of 880 and 920 °C, the 2D bands exhibited a single Lorentzian fit with a full width of half maximum (FWHM) of approximately 50.9  $\text{cm}^{-1}$  and 51.0  $\text{cm}^{-1}$ , respectively, as shown in Figure 22b.

The combination of pre-polishing and EP processes improved the surface smoothness, which is crucial for promoting the growth of high-quality graphene films on Cu foils. This highlights the importance of careful substrate preparation to achieve desirable surface characteristics, ultimately enhancing the quality and properties of the resulting graphene films.

Graphene films were grown on Cu foils using DLI-CVD with cyclohexane as the precursor and nitrogen as the carrier gas. Precise control of the cyclohexane flow rate was achieved through a direct liquid injection vaporizer. The effect of annealing temperature on graphene film quality was investigated, while the annealing time for all samples remained fixed at 10 minutes.

Micro Raman spectroscopy was employed at room temperature, utilizing a 473-nm excitation laser wavelength, to analyze the samples. The intensity of the dominant Raman peaks at the D, G, and 2D bands was measured to assess the impact of annealing temperature for a fixed annealing time of 10 minutes. The D peak intensity is related to defects in carbon materials, while the G peak corresponds to in-plane vibrational modes of  $\text{sp}^2$  carbon atoms. The 2D band reflects the stacking order of graphene layers, and the intensity ratio of the 2D peak to the G peak ( $I_{2D}/I_G$ ) indicates the number of graphene layers. A value above 2.0 suggests a monolayer, while a value below 2.0 indicates a few or multiple layers. The intensity ratio of the D

peak to the G peak ( $I_D/I_G$ ) provides information about disorder or defects in graphene [41, 42].

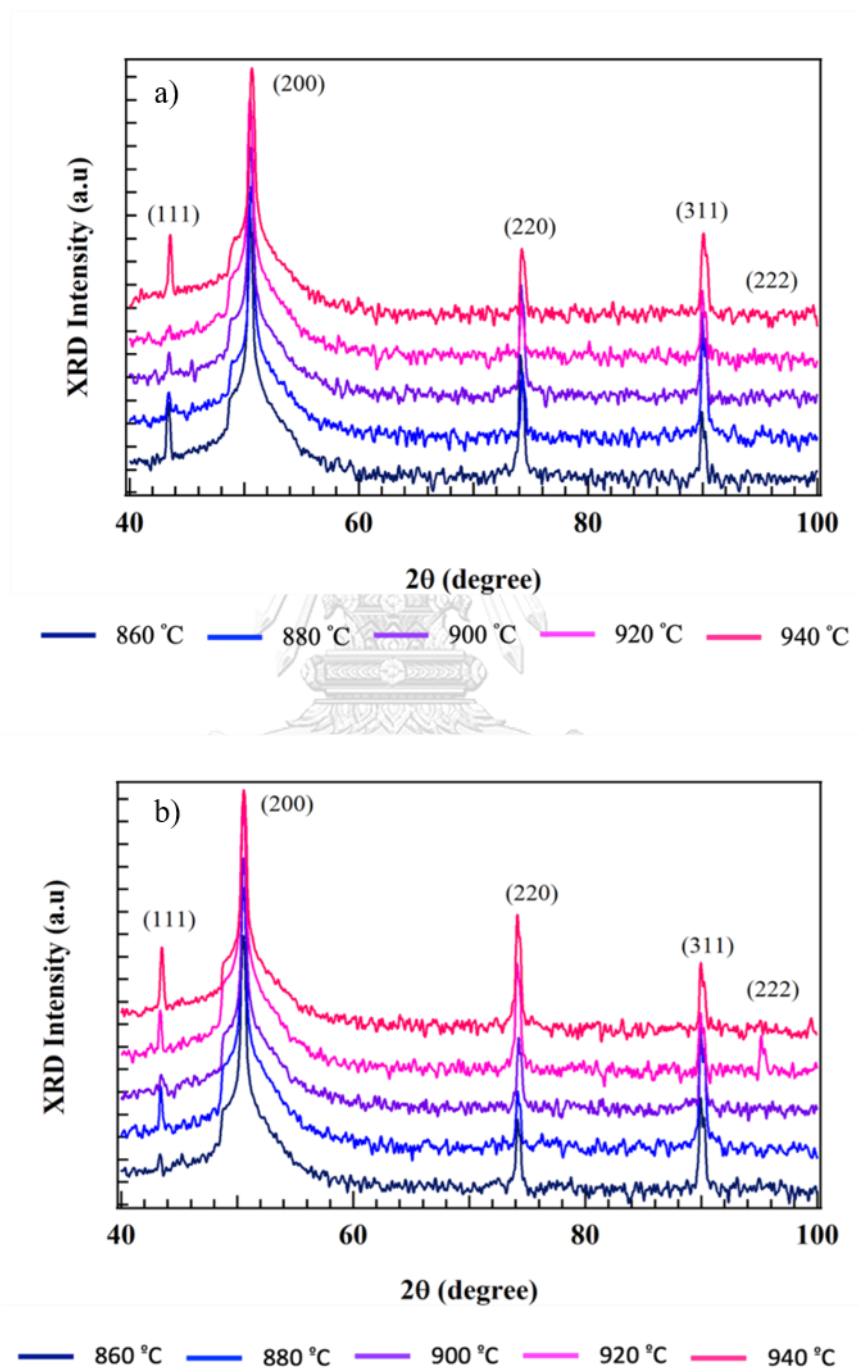


**Figure 20** Crystal orientation of Cu foil substrate: a) XRD intensity of Cu foil at different annealing temperatures, b) XRD intensity of Cu foil after the growth process with the same annealing temperature.

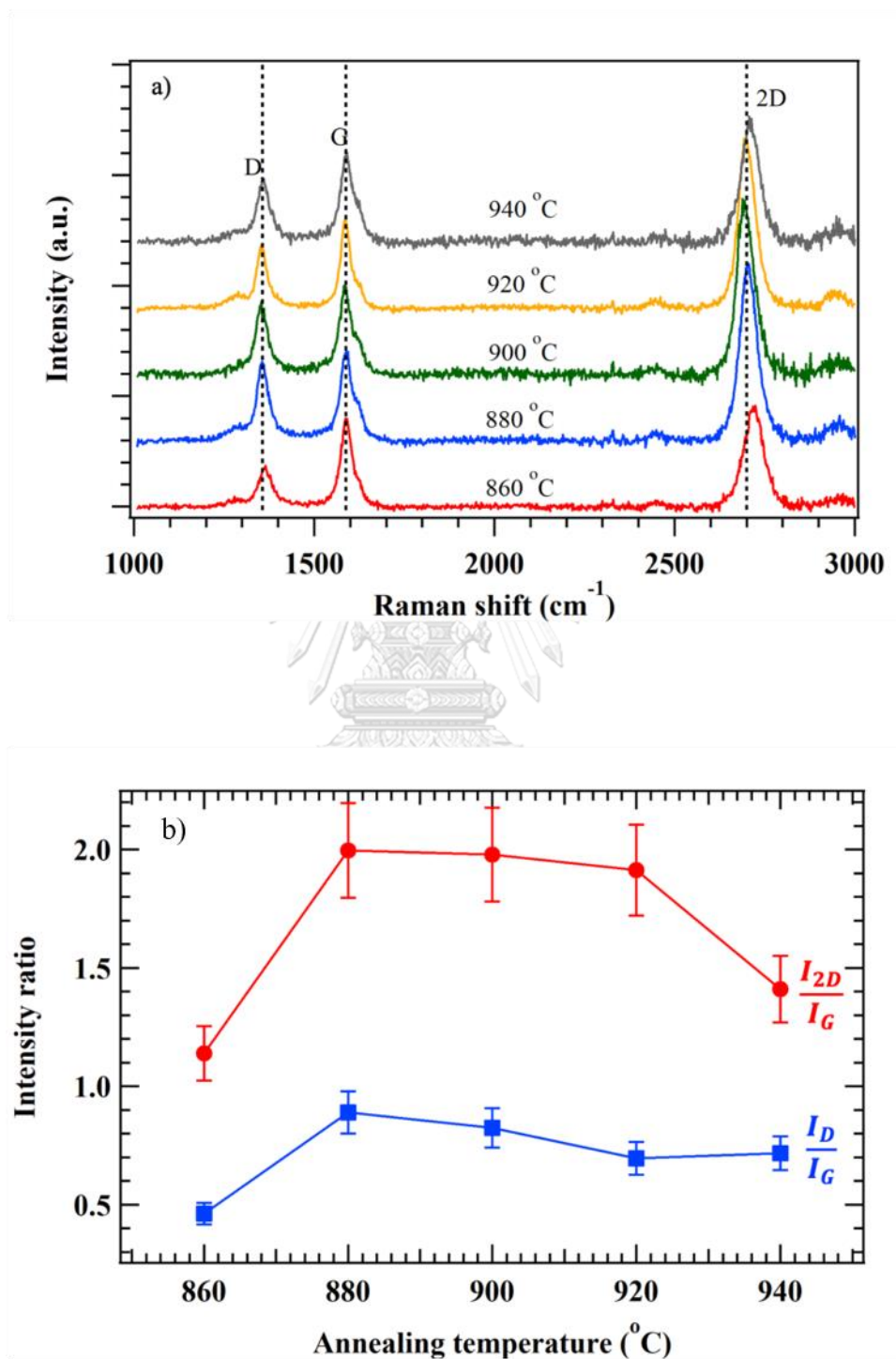


**Figure 21** Raman results of graphene on treated Cu foil: a) Graphene peaks at different annealing temperatures, b)  $I_{2D}/I_G$  and  $I_D/I_G$  ratio at different annealing temperatures.

In Figure 23a), we present the optical image of graphene grown on Cu foil using DLI-CVD. The growth conditions involved an annealing temperature of 880 °C for 10 minutes and a growth temperature of 920 °C for 6 minutes. Two different measurement positions (1 and 2) on the graphene film are highlighted, representing different surface orientations of the Cu foil substrate. The grain size of the annealed copper foil substrate exceeds 100  $\mu\text{m}$ .

In Figure 23b), Raman spectra were collected from measurement positions 1 and 2. Clear peaks corresponding to the D, G, and 2D bands were observed at Raman shifts of approximately 1355  $\text{cm}^{-1}$ , 1590  $\text{cm}^{-1}$ , and 2700  $\text{cm}^{-1}$ , respectively. The ratio of Raman intensity ( $I_{2D}/I_G$ ) was determined to be 1.996 for position 1 and 1.872 for position 2, indicating a tendency towards monolayer graphene. However, a slightly elevated intensity of the D band peak suggests the presence of a relatively high density of defects in the graphene film. This is further supported by the high intensity ratio of D and G peaks ( $I_D/I_G$ ), which measured 0.87 for position 1 and 0.84 for position 2. The full width at half maximum (FWHM) obtained from Lorentzian curve fitting exhibited characteristic values for monolayer graphene, with FWHM of 50.9 for position 1 and 52.8 for position 2.

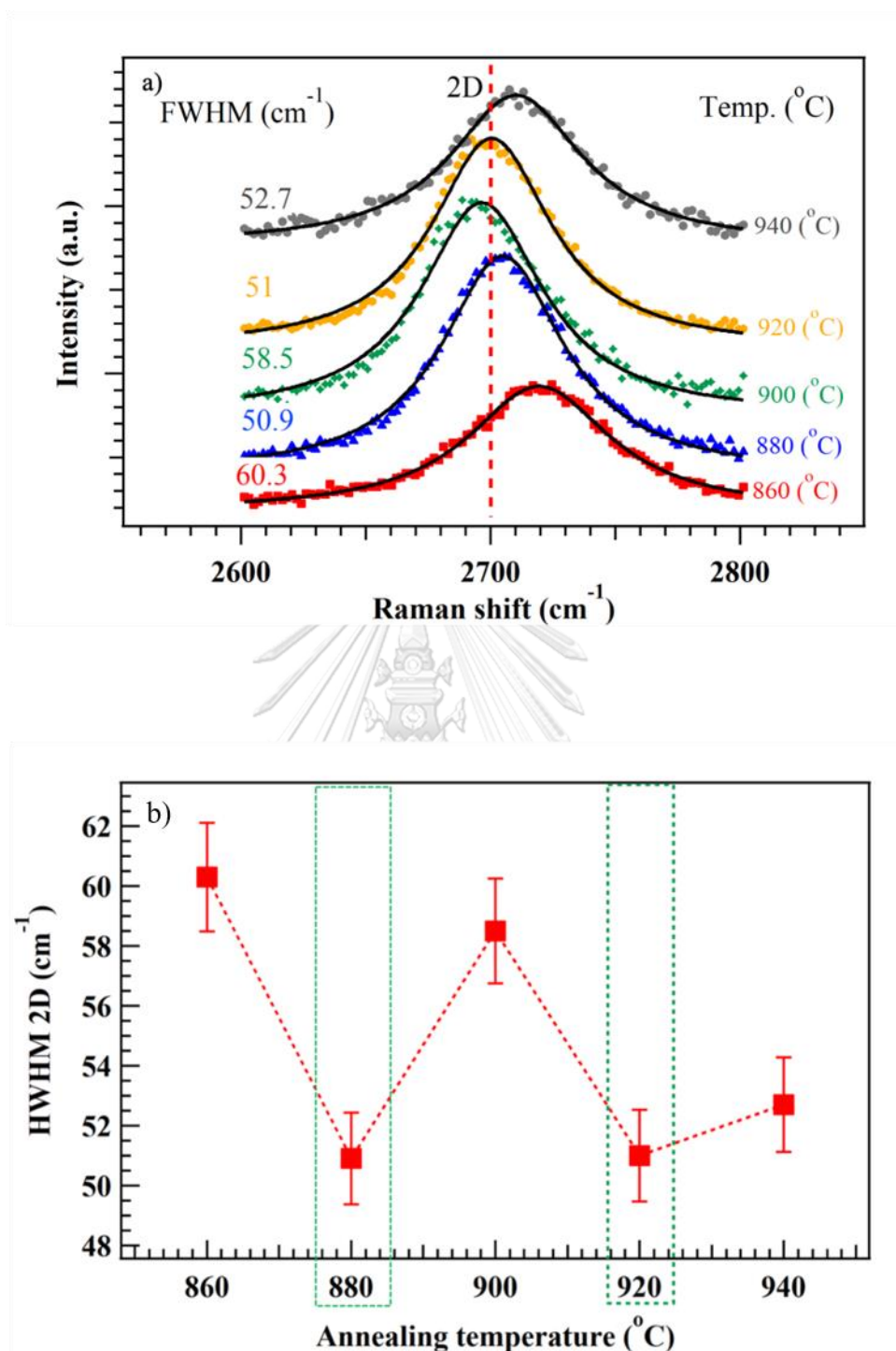


**Figure 22** Raman spectra of graphene annealed at various temperatures: a) Zoomed-in 2D peaks with single Lorentzian fit (solid black line) at different annealing temperatures, b) Full Width at Half Maximum (FWHM) of D and 2D peaks at different annealing temperatures.

Figure 24 presents the intensity ratio of  $I_{2D}/I_G$  for graphene films grown at a constant growth temperature of 920 °C. The growth time varied from 1 to 6 minutes, while different annealing temperatures ranging from 860 °C to 940 °C were applied for a fixed duration of 10 minutes. The purpose was to observe the impact of growth time on the number of graphene layers. The results showed distinct trends in the intensity ratio of  $I_{2D}/I_G$  for different annealing temperatures.

Annealing temperatures of 860 °C and 940 °C displayed a decreasing trend as the growth time extended, indicating a reduction in the monolayer character of the graphene films. Conversely, annealing temperatures of 880 °C, 900 °C, and 920 °C exhibited an increasing trend in the intensity ratio of  $I_{2D}/I_G$  with longer growth times. Notably, at an annealing temperature of 900 °C, the graphene films appeared to be more stable in terms of maintaining a monolayer structure compared to other temperatures. This stability can be attributed to the direct influence of the annealing temperature on the grain size and crystal orientation of the Cu foil surface.

These results suggest that a substantial difference between the annealing temperature and growth temperature can result in the production of multilayer graphene films, as indicated by an  $I_{2D}/I_G$  ratio lower than 2.0 after 4 minutes of growth. However, at shorter growth times, approximately 1-2 minutes, the characteristics of the graphene films seemed to exhibit greater variability. It is important to note that these results were obtained using a cyclohexane precursor with a flow rate of 0.5 g/min, which likely resulted in a higher growth rate and increased likelihood of obtaining few layers of graphene.

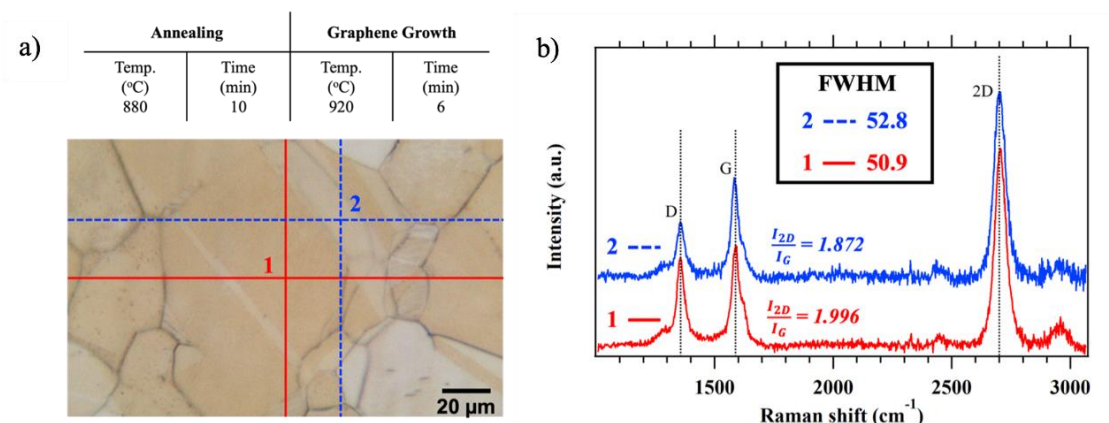


**Figure 23** Optical image of graphene film on Cu foil, showing Raman spot measurement positions (1-red solid lines and 2-blue dotted lines), along with a table displaying the temperature and time duration of annealing and graphene growth. b) Normalized Raman spectra of graphene obtained at positions 1 and 2.

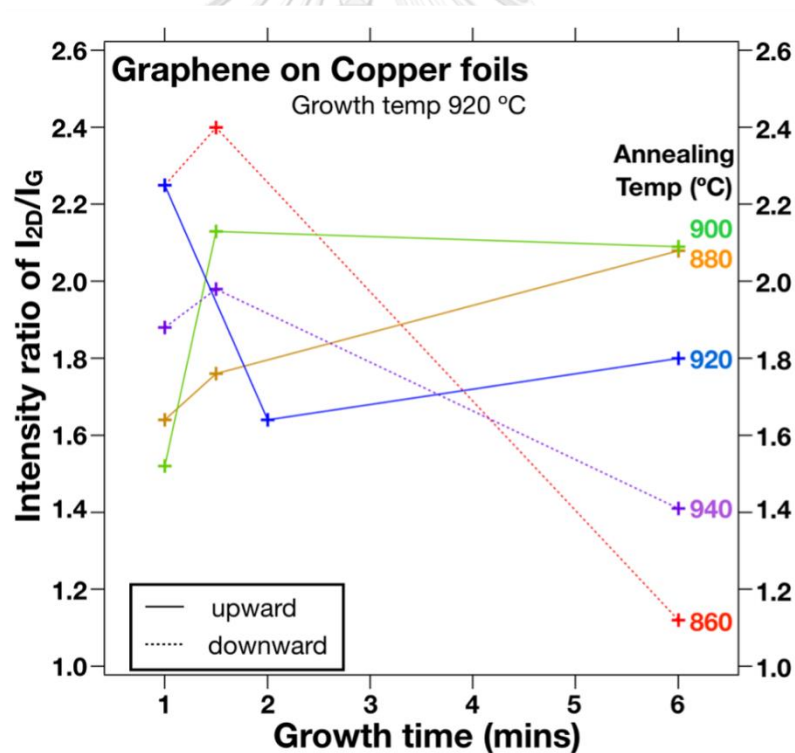


**Figure 24** Intensity ratio of 2D to G peak in graphene films on Cu foils as a function of growth time (1 to 6 minutes) at different annealing temperatures.

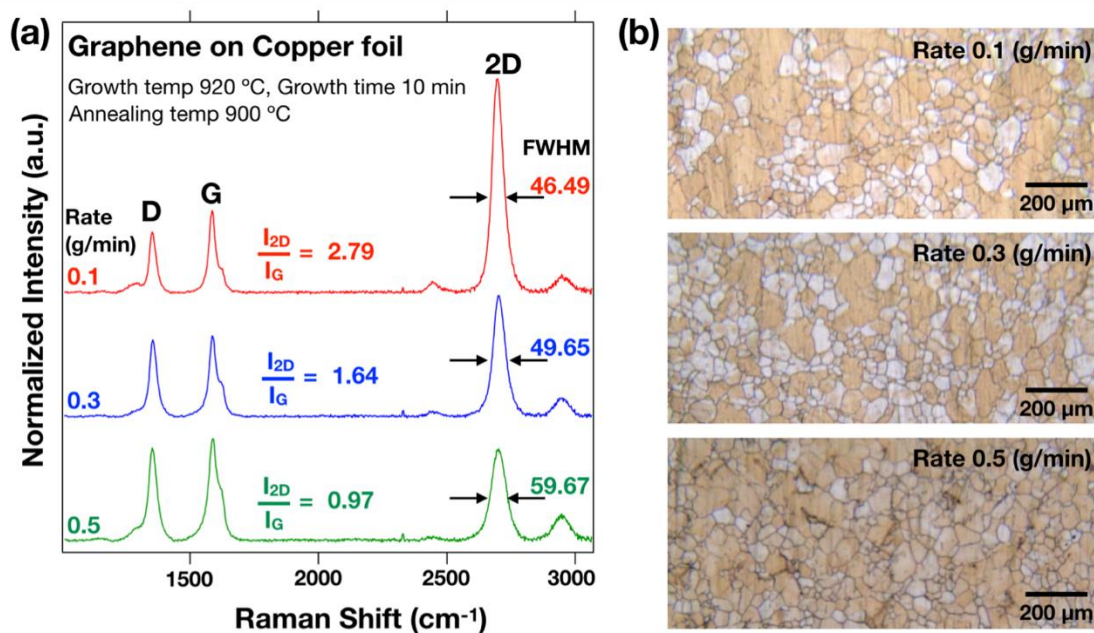
To optimize the number of graphene layers, precise control of the cyclohexane precursor flow rate was essential. Higher flow rates have been known to produce graphene films with multiple layers and higher defect densities [44]. To investigate this, graphene films were grown at a fixed growth temperature of 920 °C for 10 minutes, and annealed at 900 °C for 10 minutes, while varying the cyclohexane flow rates from 0.5 to 0.1 g/min. To observe the effect of the cyclohexane flow rate, a longer growth time of 10 minutes was chosen since lower flow rates are expected to result in a slower growth rate.

Figure 25a) illustrates that reducing the cyclohexane flow rate can significantly enhance the quality of the grown graphene films, leading to improved crystallinity as evidenced by a decreased full width at half maximum (FWHM) from 59.67 to 46.49  $\text{cm}^{-1}$ . Moreover, by decreasing the flow rate from 0.5 to 0.1 g/min, the number of graphene layers was successfully adjusted from multilayers ( $I_{2D}/I_G = 0.97$ ) to a desirable monolayer state ( $I_{2D}/I_G = 2.79$ ). However, the impact of varying cyclohexane flow rate on defects in graphene, as indicated by the intensity ratio of  $I_D/I_G$ , was less pronounced and consistently remained below 1.0 regardless of the flow rate used.

Figure 25b) displays the optical images of graphene films on Cu foils grown at different cyclohexane flow rates. Higher flow rates exhibited a dark brown color, whereas lower flow rates showed a light brown color. The optical observations, in conjunction with Raman scattering results, clearly demonstrate that lowering the cyclohexane flow rate effectively controls the number of graphene layers. However, our study did not confirm a significant reduction in defect formation during graphene



growth, as indicated by the consistently low intensity ratio of ID/IG, which remained below 1.0 and showed minimal influence from the synthesis process.



**Figure 25** Raman spectra of graphene films on Cu foils at various flow rates (0.1, 0.3, and 0.5 g/min) of cyclohexane. b) Optical images of graphene films on Cu foils corresponding to different flow rates (0.1, 0.3, and 0.5 g/min) of cyclohexane.

## CHAPTER V

### CONCLUSION

#### 5.1 Conclusion

This work focused on optimizing the growth of high-quality graphene films on thin copper (Cu) foils through various pretreatment processes and precise control of growth conditions. The pretreatment processes involved physical polishing (PP) with Brasso to smoothen the substrate surface and electropolishing (EP) with different concentrations of phosphoric acid ( $\text{H}_3\text{PO}_4$ ) to reduce rolling lines and surface contamination. The optimal conditions for substrate preparation were found to be PP and EP with 45%  $\text{H}_3\text{PO}_4$  concentration and 90 seconds etching.

The graphene films were grown on Cu foils using direct-liquid-injection chemical-vapor deposition (DLI-CVD) with cyclohexane as the precursor and nitrogen as the carrier gas. The growth conditions, such as annealing temperature and cyclohexane flow rate, were carefully controlled to achieve desirable graphene film properties.

Raman spectroscopy was used to analyze the graphene films, revealing the number of graphene layers and the presence of defects. Annealing temperature was found to play a crucial role in controlling the number of graphene layers, with temperatures around 880 °C to 900 °C favoring monolayer graphene films. Lowering the cyclohexane flow rate during growth also contributed to improving graphene film quality, resulting in fewer graphene layers and enhanced crystallinity.

While the pretreatment processes and growth conditions were optimized, defect formation during graphene growth remained a challenge. Nevertheless, this

study provided valuable insights into the synthesis of high-quality graphene films on Cu foils, highlighting the significance of substrate preparation and growth conditions in achieving desirable surface characteristics and film properties. The knowledge gained from this work contributes to the advancement of graphene synthesis for various applications.





จุฬาลงกรณ์มหาวิทยาลัย  
**CHULALONGKORN UNIVERSITY**

## REFERENCES

1. Yang, G., et al., *Structure of graphene and its disorders: a review*. Science and technology of advanced materials, 2018. **19**(1): p. 613-648.
2. Pop, E., V. Varshney, and A.K. Roy, *Thermal properties of graphene: Fundamentals and applications*. MRS bulletin, 2012. **37**(12): p. 1273-1281.
3. Blake, P., et al., *Graphene-based liquid crystal device*. Nano letters, 2008. **8**(6): p. 1704-1708.
4. Zhang, Y., et al., *Photonics and optoelectronics using nano-structured hybrid perovskite media and their optical cavities*. Physics Reports, 2019. **795**: p. 1-51.
5. Zhan, B., et al., *Graphene field-effect transistor and its application for electronic sensing*. Small, 2014. **10**(20): p. 4042-4065.
6. Avouris, P., *Graphene: electronic and photonic properties and devices*. Nano letters, 2010. **10**(11): p. 4285-4294.
7. Qin, S., et al., *Superconductivity at the two-dimensional limit*. Science, 2009. **324**(5932): p. 1314-1317.
8. Kalita, G., K. Wakita, and M. Umeno, *Low temperature growth of graphene film by microwave assisted surface wave plasma CVD for transparent electrode application*. Rsc Advances, 2012. **2**(7): p. 2815-2820.
9. Saeed, M., et al., *Chemical vapour deposition of graphene—Synthesis, characterisation, and applications: A review*. Molecules, 2020. **25**(17): p. 3856.
10. Li, X., et al., *Large-area synthesis of high-quality and uniform graphene films on copper foils*. science, 2009. **324**(5932): p. 1312-1314.
11. Guermoune, A., et al., *Chemical vapor deposition synthesis of graphene on copper with methanol, ethanol, and propanol precursors*. Carbon, 2011. **49**(13): p. 4204-4210.
12. Kang, C., D.H. Jung, and J.S. Lee, *Atmospheric pressure chemical vapor deposition of graphene using a liquid benzene precursor*. Journal of nanoscience and nanotechnology, 2015. **15**(11): p. 9098-9103.
13. Dai, G.-P., P.H. Cooke, and S. Deng, *Direct growth of graphene films on TEM nickel grids using benzene as precursor*. Chemical Physics Letters, 2012. **531**: p. 193-196.
14. Bautista, C. and D. Mendoza, *Multilayer graphene synthesized by CVD using liquid hexane as the carbon precursor*. arXiv preprint arXiv:1109.1318, 2011.
15. Gan, W., et al., *A ternary alloy substrate to synthesize monolayer graphene with liquid carbon precursor*. ACS nano, 2017. **11**(2): p. 1371-1379.
16. Campos-Delgado, J., et al., *CVD synthesis of mono-and few-layer graphene using alcohols at low hydrogen concentration and atmospheric pressure*. Chemical Physics Letters, 2013. **584**: p. 142-146.
17. Yang, J., et al., *Direct-liquid-evaporation chemical vapor deposition of smooth, highly conformal cobalt and cobalt nitride thin films*. Journal of Materials Chemistry C, 2015. **3**(46): p. 12098-12106.
18. Levush, S., S. Abadzhev, and V. Shevchuk, *Pyrolysis of cyclohexane*. Petroleum Chemistry USSR, 1969. **9**(3): p. 185-191.
19. Celebi, K., et al., *Observations of early stage graphene growth on copper*. Electrochemical and Solid-State Letters, 2011. **15**(1): p. K1.
20. Costa, S.D., et al., *Temperature and face dependent copper-graphene*

- interactions*. Carbon, 2015. **93**: p. 793-799.
21. Carlsson, J.O. and P.M. Martin, *Chemical vapor deposition. Handbook of Deposition Technologies for films and coatings*. Science, Technology and Applications, 2010: p. 444-445.
  22. Vlassioux, I., et al., *Large scale atmospheric pressure chemical vapor deposition of graphene*. Carbon, 2013. **54**: p. 58-67.
  23. Rao, R., K. Weaver, and B. Maruyama, *Atmospheric pressure growth and optimization of graphene using liquid-injection chemical vapor deposition*. Materials Express, 2015. **5**(6): p. 541-546.
  24. Ibrahim, A., et al., *Effects of annealing on copper substrate surface morphology and graphene growth by chemical vapor deposition*. Carbon, 2015. **94**: p. 369-377.
  25. Müller, F., et al., *Epitaxial growth of graphene on single-crystal Cu (111) wafers*. 2018.
  26. Intaro, T., et al. *Effect of Chemical Treatment and Thermal Annealing in N2 Atmosphere on Copper Foil Surface for Graphene Growth by Direct-Liquid-Injection Chemical Vapor Deposition Process*. in *Journal of Physics: Conference Series*. 2022. IOP Publishing.
  27. Intaro, T., et al., *Characterization of graphene grown by direct-liquid-injection chemical vapor deposition with cyclohexane precursor in N2 ambient*. Diamond and Related Materials, 2020. **104**: p. 107717.
  28. Frank, O., et al., *Interaction between graphene and copper substrate: The role of lattice orientation*. Carbon, 2014. **68**: p. 440-451.
  29. Gray, D., A. McCaughan, and B. Mookerji, *Physics for solid state applications. Crystal Structure of Graphite, Graphene and Silicon*, 2009. **6**(730): p. 1-3.
  30. Li, X., *Mechanochemical Synthesis of Carbon and Carbon Nitride Nanowire Single Crystals*. 2018: The Pennsylvania State University.
  31. Gong, C.-M., Z.-R. Li, and X.-Y. Li, *Theoretical kinetic study of thermal decomposition of cyclohexane*. Energy & fuels, 2012. **26**(5): p. 2811-2820.
  32. Yang, G., et al., *Electropolishing of surfaces: theory and applications*. Surface Engineering, 2017. **33**(2): p. 149-166.
  33. Taha, A., et al., *The effect of surfactants on the electropolishing behavior of copper in orthophosphoric acid*. Applied surface science, 2013. **277**: p. 155-166.
  34. Basko, D., S. Piscanec, and A. Ferrari, *Electron-electron interactions and doping dependence of the two-phonon Raman intensity in graphene*. Physical Review B, 2009. **80**(16): p. 165413.
  35. Li, Z., et al., *Direct-liquid-injection chemical vapor deposition of nickel nitride films and their reduction to nickel films*. Chemistry of Materials, 2010. **22**(10): p. 3060-3066.
  36. Chen, X., B. Zheng, and H. Liu, *Optical and digital microscopic imaging techniques and applications in pathology*. Analytical Cellular Pathology, 2011. **34**(1-2): p. 5-18.
  37. Casiraghi, C., et al., *Raman fingerprint of charged impurities in graphene*. Applied physics letters, 2007. **91**(23).
  38. Yu, V., et al., *Raman spectroscopy of the internal strain of a graphene layer grown on copper tuned by chemical vapor deposition*. Physical Review B, 2011. **84**(20): p. 205407.

39. AZOMATERIAL, *Graphene is a unique material that contains single molecular layers of highly crystalline graphite. This material was first reported in 2004 and represents the basic structural element of carbon allotropes including carbon nanotubes, graphite and fullerenes.* 2021.
40. Casiraghi, C., et al., *Raman spectroscopy of graphene edges.* Nano letters, 2009. **9**(4): p. 1433-1441.
41. Ferrari, A.C., et al., *Raman spectrum of graphene and graphene layers.* Physical review letters, 2006. **97**(18): p. 187401.
42. Tu, Z., et al., *Controllable growth of 1–7 layers of graphene by chemical vapour deposition.* Carbon, 2014. **73**: p. 252-258.
43. Park, J., et al., *G' band Raman spectra of single, double and triple layer graphene.* Carbon, 2009. **47**(5): p. 1303-1310.





จุฬาลงกรณ์มหาวิทยาลัย  
**CHULALONGKORN UNIVERSITY**



## VITA

<b>NAME</b>	Methawut Sirisom
<b>DATE OF BIRTH</b>	27 February 1997
<b>PLACE OF BIRTH</b>	Udon Thani
<b>INSTITUTIONS ATTENDED</b>	B.sc
<b>HOME ADDRESS</b>	119/110 wutthakat 13 Thonburi Bangkok 10600
<b>PUBLICATION</b>	SIAM PHYSICS CONGRESS (17th) at Suranaree University of Technology. Journal of Material Science (JMSC)
<b>AWARD RECEIVED</b>	-



จุฬาลงกรณ์มหาวิทยาลัย  
CHULALONGKORN UNIVERSITY